SEMMELWEIS EGYETEM

DOKTORI ISKOLA

Ph.D. értekezések

3471.

SEBASTIAN ANDREAS GSCHWINDT

Fogorvostudományi kutatások

című program

Programvezető: Dr. Varga Gábor, egyetemi tanár

Témavezető: Dr. Arvin Shahbazi Irani, egyetemi adjunktus

Integrated Vascular Architecture of the Hard Palate and Musculovascular Organization of the Upper Lip: Surgical Relevance in Cleft Reconstruction

Ph.D. Thesis

Sebastian Andreas Gschwindt D.M.D., M.D.

Dental Research Division

Semmelweis University

Supervisor:	Arvin Shahbazi Irani D.M.D., Ph.D.
Official reviewers:	Tamás Huszár M.D., Ph.D.
	Kristóf Boa M.D., Ph.D.

Head of the Complex Examination Committee:	Gábor Gerber D.M.D., Ph.D.
Members of the Complex Examination Committee:	Beáta Kerémi D.M.D., Ph.D.
	Andrea Radácsi D.M.D., Ph.D.

Budapest
2026

“As the Hungarian proverb ‘Nagy sebész, nagy metszés’ reminds us—skill is not proven by a large incision. The refined surgeon chooses the smallest cut necessary.”

Table of Content

List of Abbreviations

ANM	Alar part of nasalis muscle
CCA	Common carotid artery
CT	Computed tomography
DNA	Dorsal nasal artery
DSNM	Depressor septi nasi muscle
ECA	External carotid artery
FA	Facial artery
GPA	Greater palatine artery
ILSM	Incisivus labii superioris muscle
IOA	Infraorbital artery
LLSANM	Levator labii superioris alaeque nasi muscle
LLSM	Levator labii superioris muscle
LPA	Lesser palatine artery
MM	Myrtiformis muscle
MMS	Myrtiform muscular system
MRI	Magnetic resonance imaging
NM	Nasalis muscle
NPA	Nasopalatine artery
OOM	Orbicularis oris muscle
PSAA	Posterior superior alveolar artery
PSB	Philtral septal branches
SAB	Subalar branch
SLA	Superior labial artery
SMAS	Superficial musculoaponeurotic system
SPA	Sphenopalatine artery
TNM	Transverse part of nasalis muscle

1. Introduction

Accurate wound healing is fundamental to the success of surgical interventions, particularly in the aesthetic region of the face, where primary wound healing via optimal angiogenesis is essential to minimize complications such as haemorrhage, infections, necrosis and excessive scarring (1, 2). Appropriate design of surgical flaps and incisions directly influences vascularization and healing outcomes, presenting specific challenges in maxillofacial surgeries. In cleft repair, multiple staged interventions are often required at different times, which may interfere with maxillary growth and long-term functional development (3, 4). Potential long-term complications include secondary deformities or dehiscence of the lip and nose, palatal fistula formation, necrosis and auditory dysfunction (2, 5–7). Furthermore, velopharyngeal insufficiency may lead to inadequate ventilation, snoring, and speech disorders by hypernasality. Consequently, detailed knowledge of the non-cleft anatomy, neurovascular pathways and musculature is fundamental for restoring physiological function and aesthetic harmony in cleft surgery.

Clefts affect approximately one in 700 live births worldwide (8), with the highest incidence in reported in Asian- and the lowest in African populations (9, 10). Although, the aetiology remains incompletely understood, accumulating evidence indicates that genetic, environmental, and ethnic factors contribute to cleft formation (10–21). To understand how these influences manifest, it is essential to first consider the normal upper-lip anatomy. In non-cleft individuals, the upper lip is bordered superiorly by the nasal base and alar sulci and laterally by the nasolabial folds.

The upper lip is primarily composed of the orbicularis oris muscle (OOM), which unites with the lower lip at the oral commissure and functions in coordination with the levator labii superioris (LLSM), levator labii superioris alaeque nasi (LLSANM), risorius, zygomatic, depressor anguli oris, levator anguli oris, nasalis and buccinator muscles to regulate facial expressions and oral competence (22–27). Structurally, the upper lip is divided into the central philtral subunit and two lateral subunits. The philtrum defines the contour of the upper lip and forms the Cupid´s bow above the lip vermillion (28). The philtral columns arise from the ipsilateral interdigitating fibres of the levator alaeque nasi muscle and the peripheral portion of the OOM (24). Briedis and Jackson described the bilaminar organization of the OOM consisting of a continuous deep and a superficial

decussating layer inserting into the contralateral philtral column and dermis (29). Nicolau, further subdivided the superficial layer into upper and lower bundles, with the lower nasolabial bundle receiving fibres from the depressor anguli oris muscle (23). Long fibres contribute to the contralateral philtral column, whereas short fibres reinforce the ipsilateral philtral column, explaining the characteristic thickness of the the philtral columns (30, 31). The vermilion represents the transitional zone between keratinized skin and non-keratinized oral mucosa, marked by disappearance of the stratum granulosum (29, 30, 32).

Beneath the OOM at the level of the apex of the upper lateral incisor of the anterior maxilla lies the myrtiform fossa, which serves as the origin of several nasolabial muscles, that have historically been described using different terminologies (33–41). The musculature arising from this region counteracts the muscle function of LLSM and LLSANM, contributing to inferomedial positioning of the lateral nasal cartilage and the inferior displacement of the nasal septum as proposed by Yegi et al. (34). Furthermore, the authors highlighted the connection between the depressor septi nasi muscle (DSNM) and myrtiformis muscle (MM) (34). De Souza Pinto (35) described the MM as the lateral portion of the DSNM, while Uzmansel and Öztürk identified three morphological variants, based on single- or double muscle bellies (36). The single-belly type was most common which presented two subtypes; subtype 1 (80%) with fibres inserting at the nasal base and nasal septum, and subtype 2 (10%) inserting to nasal septum, nasal base and nasal wing. The double-bellied muscle (10%) attached with a medial belly to the nasal septum and a lateral belly into the nasal floor. The authors suggested that the combined DSNM and the lateral depressor alae nasi muscle together constitute the MM with interdigitations into the OOM (36). Similarly, Figallo et al. differentiated inner fibres corresponding to the DSNM from the outer fibres of the depressor alae nasi muscle, with connections to the OOM and the labial fibres of the LLSANM (37). Rohrich et al. classified the DSNM and its connection to OOM fibres (38), whereas Daniel et al. reported consisted presence of the DSNM without such connections (42). In cleft anatomy, Delaire applied the term MM to refer to the inferior component of the transverse part of nasalis muscle (TNM) (43). Despite these observations, anatomical terminology remains inconsistent when referring to the DSNM, depressor alae nasi, or MM originating from the myrtiform fossa. It is unclear whether these represent variations of a single

muscle or distinct, coexisting structures. From an embryologic perspective, cleft lip and alveolus result from failed fusion of the maxillary and nasal prominences, impacting the osseous morphology of the myrtiform fossa, leading to impaired premaxillary growth, due to abnormal tooth eruption, tongue pressure, deviated muscle vectors and occlusal forces (44, 45). The nasolabial muscles exhibit displaced insertions, affecting the planar arrangement of the anatomical subunits of the lateral cleft margins, such as the, cheek, nasal sill and nostril (46).

These developmental disturbances also intersect with significant alterations in the vascular development. The orofacial region receives its blood supply primarily from branches of the facial- (FA) and maxillary artery, both branches of the external carotid artery (ECA) (47, 48). This follows the embryological transition from the internal carotid to the external carotid system and development of the first and second pharyngeal arch (49, 50). This transition in vascularization may determine the dominance of specific vessels, subsequent musculoskeletal development and hence prominence fusion. In cleft malformations, normal development is hindered and therefore vascularization may further be disrupted and suggests limited collateral vascularization.

The superior labial artery (SLA), a highly variable branch of the FA plays a dominant role in vascular upper lip perfusion (51, 52). It courses beneath or within the fibres of the OOM (53), giving rise to ascending branches lateral to the philtrum and septal branches supplying the nasal septum through deep and a superficial plane (54–58). Additional, vascular contributions arise from the infraorbital artery (IOA) and branches of the ophthalmic artery to supply the nostrils and nasal septum (58, 59).

As previously outlined, cleft formation results from failure of fusion between the maxillary and frontonasal prominences, more detailed, the medial nasal prominence (44, 45, 49). From an intraoral developmental perspective, the frontonasal prominence gives rise to the intermaxillary segment, which comprises a labial component (forming the philtrum), an upper jaw component (bearing the four incisor teeth), and a palatal component (forming the triangular primary palate) (44, 49). The secondary palate develops from bilateral outgrowths of the maxillary prominences, forming palatal shelves that initially extend obliquely downward alongside the tongue before elevating and fusing at the midline. Disruption of these coordinated fusion processes—either between the primary and secondary palate or between the secondary palatal shelves—results in clefts

involving the anterior hard palate and, respectively, the posterior hard and soft palate (44, 45, 49). Such defects may extend to the alveolar process and palate, significantly altering oral and facial architecture. From a morphological perspective, the palate is divided into the anterior hard palate and the posterior soft palate; sometimes, the aperture of palatal glands can be found with two small palatine foveas at the border (60). The hard palate is formed by the premaxilla, the palatine process of the maxillary bone and the horizontal plates of the palatine bones, which contain the greater and lesser palatine foramina. In the midline of the palate runs the palatine raphe, which is limited within the premaxilla by the nasopalatine foramen and its canal (61). The nasopalatine artery (NPA), the terminal branch of the sphenopalatine artery (SPA) traverses the nasopalatine canal to supply the anterior palate (62). Posteriorly, the descending palatine artery divides into the greater palatine (GPA) and lesser palatine (LPA) arteries as it enters or courses within the greater palatine canal (63–65). After emerging through the greater palatine foramen, between the second and third molars, the GPA courses anteriorly within the lateral palatine groove to anastomose with the NPA. The lateral palatine groove is separated from the medial palatine groove by the palatine ridge (66, 67).

Various vascular studies of the hard palate have been reported in the literature. Yu et al. described four branching patterns of the GPA in relation to the palatine ridge morphology, most commonly observing bifurcation into medial and lateral branches after crossing the ridge (68). A supplementary branch to the canine was consistently identified, usually arising from the lateral branch. Blakeway and Shahbazi et al. detected extraosseous anastomoses between bilateral GPAs, likely representing connections between the medial branches (69, 70). Reiser et al. reported variable distances of the GPA from the palatal gingival margin depending on palatal vault height, emphasizing the importance of individualized incision planning (71). Morphological variation is further influenced by dentition status and bone resorption in edentulism, as well as developmental changes in children (68, 72). Rossell-Perry identified altered greater palatine foramen morphologies in cleft palates, including duplication, absence, vascular hypoplasia and malposition (73). It is well known that branches of the palatal NPA/GPA vascular network supplies not only the palatal mucoperiosteum but also the alveolar ridge and interdental septa (74, 75). Additional collateral circulation arises from ascending palatine and the ascending pharyngeal artery (76, 77).

Although detailed knowledge of palatal vascular anatomy is critical for surgical safety, vascular patterns may deviate in cleft malformations, necessitating awareness of collateral pathways. Various in vivo imaging techniques—including micro computed tomography (CT), fluoroscopy, angiography, laser Doppler, and laser speckle imaging—have been employed to study vascular perfusion (58, 78–81). While these methods provide functional data on blood flow dynamics, they offer limited visualization of precise anatomical vessel courses and fail to depict intraosseous vascular pathways. Micro-CT offers improved morphological resolution but remains minimally invasive and resource intensive (59, 82).

Consequently, ex vivo techniques have become essential for comprehensively mapping musculovascular relationships in both soft and hard tissues, thereby facilitating improved surgical planning and reconstruction.

2. Objectives

The aim of this PhD dissertation is to characterize the extra- and intraosseous vascular anastomoses of the hard palate and the nasolabial region, and to translate these anatomical findings into clinically relevant recommendations for incision and flap design in cleft repair. Although cleft surgery has a long-standing history with numerous established techniques, the detailed vascular anatomy of the hard palate and the musculovascular morphology of the myrtiform area in cleft individuals remains incompletely understood. Furthermore, data derived from cleft specimens are limited due to the ethical and practical constraints associated with cadaveric research in this population.

This dissertation addresses two primary research questions:
(1) How are the intra- and extraosseous vascular anastomoses of the hard palate organized, and how can incision and flap design be optimized to preserve these collateral pathways in patients with cleft palate?
(2) How does the arrangement of nasolabial musculature and its associated vascular supply influence surgical strategies in cleft lip-nose repair?

To address these questions, a comprehensive review of the literature was conducted, focusing on the hard palate and the myrtiform area, with particular emphasis on their surgical relevance in cleft reconstruction. This was followed by detailed anatomical investigations, including dissection and analysis of 36 adult and 4 fetal cadaveric specimens, to characterize regional vascular and muscular patterns and their variations. The findings were subsequently interpreted in collaboration with international cleft surgeons from multiple institutions to develop refined surgical concepts aimed at preserving morphological integrity.

By integrating detailed anatomical insights with clinical considerations, our research aimed to optimize surgical maneuver to improve functional and aesthetic outcomes and reduce complications during and after cleft surgery.

3. Material and Methods

The research presented in this dissertation is based on human cadaveric studies conducted entirely at the Department of Anatomy, Histology and Embryology of Semmelweis University, Budapest, Hungary. The anatomical dissections were systematically evaluated and correlated with clinical observations through interdisciplinary collaboration with surgeons from the University of Bern (Bern, Switzerland), University of Basel (Basel, Switzerland), Lokman Hekim University (Ankara, Türkiye), and the University of Melbourne (Melbourne, Australia). This integrative approach facilitated the refinement of a surgically relevant framework based on the collective interpretation of the anatomical findings.

All cadavers were donated for scientific research purposes to the Department of Anatomy, Histology and Embryology of Semmelweis University, Budapest, in accordance with Hungarian legislation on anatomical donations (approval number: 110/2020. (VII.07.)) and in compliance with the ethical principles for medical research involving human subjects as outlined by the World Medical Association (Declaration of Helsinki). The specimens were prepared and dissected using various anatomical embalming and injection techniques to analyze vascular and muscular patterns in cleft-related regions of the hard palate and upper lip. Photographic documentation was performed using a digital single-lens reflex camera (Canon 600D) equipped with a 100 mm f/2.8 macro lens and a portable flash system (Godox MS300II-D). Dissections were carried out layer by layer using No. 15 and 15C surgical blades (Swann-Morton Limited) under 2.5x–5x magnification loupes.

In the first study, intraosseous vascular pathways of the palate were analyzed in 11 adult cadaver heads (7 males, 4 females; aged 50–85 years) using the corrosion casting technique. In the second study, the collateral vascularization of the hard palate was investigated in 12 adult cadaver heads (7 males, 5 females; aged 55–90 years) and one aborted fetus (26 weeks of intrauterine age) presenting with a unilateral complete cleft of the hard and soft palate, corresponding to Group II in the Veau classification (83). The Veau classification describes four groups from posterior to anterior, with I describing the soft palate cleft and IV the complete bilateral cleft (83). The study aimed to macroscopically assess collateral circulation patterns of the hard palate. The adult

specimens were processed using the corrosion casting technique, while the cleft fetus was embalmed in formaldehyde and injected with a white-colored barium sulfate agent.
In the third study, the musculovascular anatomy of the nasolabial region was investigated in 21 adult specimens (11 males, 10 females; mean age 73 years) and 3 aborted fetuses (18, 20, and 24 weeks of intrauterine age). This study analyzed the vascular supply and muscular structures of the upper lip, philtrum, and nostril regions. The adult specimens were embalmed using formaldehyde (7 specimens), Thiel solution (10 specimens), or prepared using the corrosion casting technique (4 specimens). In the Thiel-embalmed specimens, arteries were injected with latex milk, whereas in corrosion cast specimens, acrylic resin was used. The fetal specimens were embalmed in a formaldehyde solution.

3.1. Embalming Methods

3.1.1. Formaldehyde Fixation

In 1868, the intriguing compound known as formaldehyde gas was discovered by the German chemist August Wilhelm von Hofmann (84). Following this discovery, researchers soon realized that the mixture of formaldehyde with water and methanol, referred to as formalin (85). First, it was applied as an antiseptic, before Ferdinand Blum accidentally recognized its tissue fixative properties in 1893 (85). Since then, formalin has become widely recognized for its low cost, low shrinking, effective tissue preservation and antiseptic properties (84–86).
In our study, the fresh specimens were first intraarterially perfused with a percentage of 8% formaldehyde, followed by full body immersion for one year in a 4% formaldehyde solution corresponding to 10% formalin. Fetal specimens, due to their smaller size and more delicate vasculature, were preserved solely by immersion in 4% formaldehyde without any arterial injection. The fixation process is influenced by several factors, such as time, pH, temperature, and viscosity (87). Diffusion throughout the tissue is enhanced under a higher pressure (88). This not only facilitates a more uniform distribution but also accelerates the overall fixation process. The rate of formaldehyde penetration slows down as it reacts with the tissues. Below a certain concentration level, further diffusion becomes limited and stops. This makes it necessary to replace the solutions to keep diffusion active.

These changes in movements follow the principles described by Fick's first law of diffusion, which explains how molecules spread through the tissues (87, 89).

Exposure to oxygen promotes the oxidation of formaldehyde, thus compromising the fixative capacity. Oxidation can be limited through the addition of phosphate salts, and methanol further stabilizes the solution by inhibiting condensation (89). However, the high percentage of 37% formaldehyde not only made the specimen's tissues very stiff and rigid but also provoked medical illnesses for the workers involved (90–92). It is classified as a Group 1 of carcinogens in humans (93, 94). Consequently, exposure limits are adopted by health authorities to limit nasopharyngeal cancer, ocular irritation, skin irritations and genotoxicity (95, 96).

Formaldehyde is a highly reactive electrophilic molecule known for its ability to form methylene bridges through the process of crosslinking with biological macromolecules, such as the amino acids of proteins (89, 97). Different mixtures have been further developed to counterbalance the effects of formaldehyde, preserving more natural softness and elasticity of the specimens, including methanol, ethanol, glutaraldehyde, phenol, dyes, wetting agents or other substances (98–102). For effective preservation, formaldehyde not only requires chemical cross-linking, but also needs to penetrate physically into the cells.

3.1.2. Thiel Fixation

The Austrian anatomist Walter Thiel introduced in 1992 a method to preserve the flexibility and colors in cadavers (103–105). This facilitates cadaver handling and provides realistic conditions for simulating invasive procedures with low pungent odor, due to the lesser quantity of formaldehyde (106).

The method consists of two parts using the Thiel´s injection- and immersion solution based on the above-mentioned chemicals in a different mixing ratio. Both solutions were prepared in our investigation according to the protocol of Thiel (103). In a first step, the carotid arteries were first washed meticulously with warm water before applying the injection solution. After, the complete cadaver was immersed in a metal tank containing the immersion solution for six months. Thiel, however, reported that the immersion requires only 30 days, assuming the cadaver is re-immersed weekly to avoid dryness (103,

105–107). We combined the Thiel embalming with subsequent following latex milk injections with a red color agent to demonstrate the vascular pathways in color.

Based on various studies, the immersion solution is primarily composed of solution A—a mixture of boric acid, ethylene glycol, ammonium nitrate, potassium nitrate, and hot water—and solution B, consisting of ethylene glycol and 4-chloro-3-methylphenol (103, 105, 106, 108). Solution A essentially represents a higher-concentration formulation of the main components of the immersion solution (103, 105, 106, 108), while solution B is also incorporated into the injection solution in a higher volume. The injection solution can further contain formaldehyde, sodium sulfate, and solution A.

The cadaver elasticity and flexibility after the immersion period were maintained by storage in zipper polyethylene bags, with periodic moistening using Thiel solution to preserve humidity, and by adding antifungal agents to prevent mycosis (105, 108).

The fixation technique elaborated by Thiel can be more expensive than formaldehyde embalming because of the numerous components required for its solutions (108). It also demands careful handling and specific equipment, particularly when combined with the injection of latex into the vessels. Consequently, its use remains limited, because inaccuracies may comprise the entire process. However, the tissue properties resemble those of living humans, which makes it useful in surgical training courses, where tissue properties closely resembling those of living humans are essential. The soft tissues retain a natural feel, and joint mobility may also be preserved to a certain degree, broadening the range of procedures that can be simulated under conditions close to those in the operating room.

3.2. Vascular injection methods

3.2.1. Latex injection

As mentioned in the previous chapter (3.1.2), the Thiel embalming technique was combined with arterial injection using colored latex milk to demonstrate precise vascular pathways in the head and neck region (109, 110). The staining rendered the vessels visible, even for non-experts, and proved to be an ideal method in combination with the Thiel technique for conducting surgical training courses with a focus on vascular anatomy. Latex milk is additionally radiopaque, enabling radiological three-dimensional

tracing of the injected vessels by CT (110). The common carotid artery (CCA) or ECA of cadaver heads was carefully dissected within the carotid triangles on both sides, after which the vessels were rinsed with phosphate-buffered saline to remove blood clots and subsequently flushed with Thiel injection solution, with an additional saline rinse performed when necessary. Based on the approximate vessel diameter, an appropriately sized Coude or Foley catheter was inserted and secured with fibre plastic bands to prevent leakage. Red-colored latex milk (So-Strong red color tint, Smooth-On; Creato Latexmilch, Zitzmann Zentrale) was then injected into the CCAs/ECAs using a syringe, applying consistent pressure and slightly increasing it during progression to ensure adequate perfusion of smaller and more intricate vessels. The cadaver heads were embalmed in stainless steel tanks containing Thiel solution, and because only the heads were included in this investigation, immersion time was reduced to approximately four months. Afterward, the specimens were stored in polyethylene bags with chlorocresol to inhibit mold and bacterial growth. Finally, layer-by-layer dissections were performed using No. 15 and No. 15C surgical blades (Swann-Morton Limited) under 2.5x–5x magnification to visualize arterial pathways and anastomoses within the different soft-tissue layers.

3.2.2. Corrosion Casting

The corrosion casting method is based on two successive processes to visualize the injected arteries in relation to the bone in fresh specimens.

First, during the casting phase, the CCAs/ECAs of cadavers up to two to three days post-mortem were identified and dissected. A Foley or Coude catheter was inserted and secured within the CCA/ECA to prevent leakage under pressure (111). Blood clots were removed with subsequent phosphate-buffered saline rinsing. Previous studies have shown that glutaraldehyde, formaldehyde, and paraformaldehyde can be used in varying concentrations to prevent resin leakage from the vessels into surrounding tissues (112–115). These agents may also strengthen vascular walls and limit expansion during resin injection. Acrylic resin (ACRIFIX 190 (2 R 0190), Evonik Industries AG), mixed with a red dye (AKEMI GmbH), was injected into the ECAs. The injection was performed at a controlled rate to avoid vessel rupture or incomplete filling (112, 113). Undiluted resin

was used to prevent shrinkage during polymerization. After injection through each bilateral catheter, ligatures were applied to seal the catheters. The head specimens were then maintained in a stable position to avoid deformation (111–113). After 30 minutes, the specimens were transferred to a warm water bath (40–60 °C) for 24 hours to ensure complete polymerization (112, 113).

Second, during the corrosion phase, tissue maceration was performed. The specimens were transferred from the water bath into a stainless-steel tank containing potassium hydroxide solutions at concentrations of 2–4% (116, 117). To optimize enzymatic activity, Somat Gold 12-action dishwasher tablets (Henkel AG) were used in a constant water bath at 40 °C for approximately three months. Increased temperature was associated with accelerated maceration (113). Approximately three dishwasher tablets were added to the solution every two weeks. After 2–3 months, all soft tissues were completely macerated. The specimens were then rinsed with water for 3 minutes to remove chemical residues and debris, followed by immersion in tap water for 20 minutes. Finally, the specimens were dried. Instead of freezing or incubator drying, drying was performed at room temperature (112, 113). However, as noted by Lametschwandtner et al., air drying may introduce tension within the injected vessels during evaporation, and the use of high-concentration alcohol baths has been suggested to reduce surface tension effects (113).

At the end of the process, only the injected vascular structures and the bone remained. For intraosseous arterial investigations, localized application of potassium hydroxide was employed to selectively dissolve bone, enabling three-dimensional visualization of the vascular network.

3.2.3. Barium sulfate injection

The cleft fetus was canulated and injected with white barium sulphate (Micropacque®, Guerbet GmbH) through the CCAs in order to comprehensively evaluate the macroscopical course of the vessels, while also allowing for a detailed radiological examination (118). The injection made the vessels clearly visible beneath the mucosa. It is highly stable, does not degrade, and is generally considered safe for radiological applications.

4. Results

4.1. Hard palate and alveolar arterial architecture and collateral circulation patterns in normal palate

The course of different extra- and intraosseous arterial pathways was identified using the corrosion casting technique in normal adult specimens (74, 166). In addition to the primary supply provided by the GPA-LPA-NPA, a complex vascular network was observed, suggesting the presence of collateral circulation capable of compensating in cases of vascular compromise. Both extraosseous and intraosseous patterns were identified and are described as follows:

Extraosseous vascularization:

- In the posterior portion of the palate between the maxillary tuberosity and the pterygoid hamulus, the GPA, LPA and maxillary artery formed a complex retrotuberal vascular network (Fig. 1).

Fig. 1 Retrotuberal arterial pattern. **(a)** The retrotuberal aspect of maxillary tuberosity received an intraosseous branch from the greater palatine artery (GPA) and an extraosseous branch from the lesser palatine artery (LPA). **(b)** The retrotuberal aspect of maxillary tuberosity presented complex extraosseous anastomoses between branches of GPA, LPA, and maxillary artery (MA), respectively. (166)

Intraosseous vascularization:

In both studies (74, 166), following dissolution of the bone, intraosseous anastomoses between multiple arteries were identified at the level of the alveolar ridges, hard palate, and intermaxillary suture, particularly within the region of the anterior nasal spine. This anastomotic network established collateral communication with various vascular territories, especially the premaxilla, vestibular aspect, and nasal cavity:

- Intraosseous anastomoses were formed between branches of the bilateral IOAs, which connected with the NPA and GPA in the premaxilla (Fig. 2).
- Vertico-oblique intraosseous anastomoses (vertico-oblique loop): connections between branches of posterior superior alveolar artery (PSAA)/IOA and the GPA revealed after maceration of the anterolateral maxillary wall and alveolar crest (Fig. 3).
- Horizontal bony perforating anastomoses (transverse loop): transverse connections between GPA branches and PSAA/IOA branches located in the interdental septum and alveolar crest. Arterial perfusion exhibited a palatal-to-buccal directionality. Around the alveolar socket, intraseptal branches of this loop formed a vascular network, which were also observed in various dental status (Fig. 4).
- In the middle portion of the median palatine suture, a larger penetrating artery is formed by the anastomosis of the bilateral GPAs (Fig. 5).
- The anterior and middle portion of the palate, mainly at the height of the premolar area, is perforated by branches of the GPA. These branches traversed the palatine process of the maxilla and anastomosed with the posterior septal nasal branches (branches of the SPA) at the floor of the nasal cavity. The alveolar ridge territory is mainly supplied by intraosseous branches of the IOA (Fig. 6).

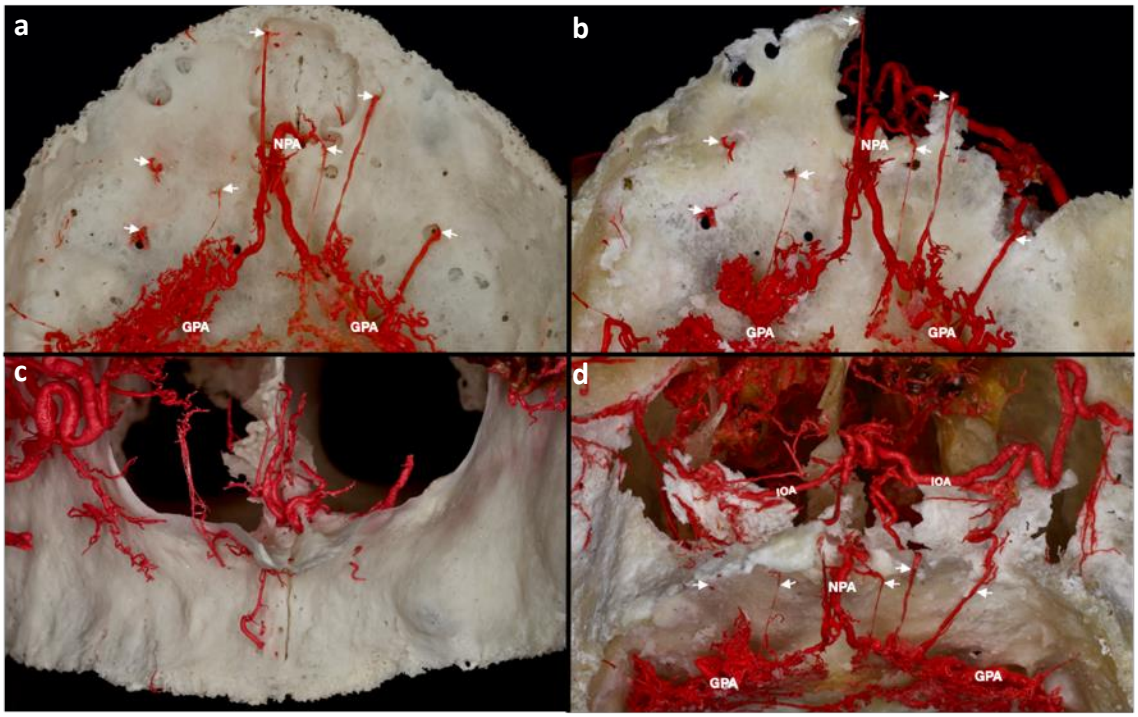

Fig. 2 Intraosseous arterial anastomoses of the premaxilla. **(a)** Premaxilla (inferior view) without maceration of the hard tissue, arrows (↑) indicate the intraosseous branches of the greater palatine arteries (GPA) and the nasopalatine artery (NPA). **(b)** After hard tissue maceration, the premaxilla (inferior view) displays the intraosseous branches of the GPA/NPA that establish anastomoses with the infraorbital artery (IOA). **(c)** Premaxilla (anterior view) without hard tissue maceration, indicates the arterial network emerging behind the anterior nasal spine. **(d)** Premaxilla (anteroinferior view) with hard tissue maceration, the bilateral IOAs form complex anastomoses and circulation with the GPA/NPA. (166)

Fig. 3 Vertico-oblique intraosseous anastomoses (vertico-oblique loop). **(a)** Anterolateral view of the maxilla, vertico-oblique intraosseous branches of the infraorbital artery (IOA), and the greater palatine artery (GPA), concealed in the anterolateral surface of the maxilla. **(b)** Anterolateral view of the maxilla with a magnified view. After removing the hard tissue through the cautious maceration, vertico-oblique loop between IOA and GPA in the alveolar crest and socket initiated the arterial network. **(c)** Inferior view from the side of the hard palate; the anastomoses are marked with arrows. (74)

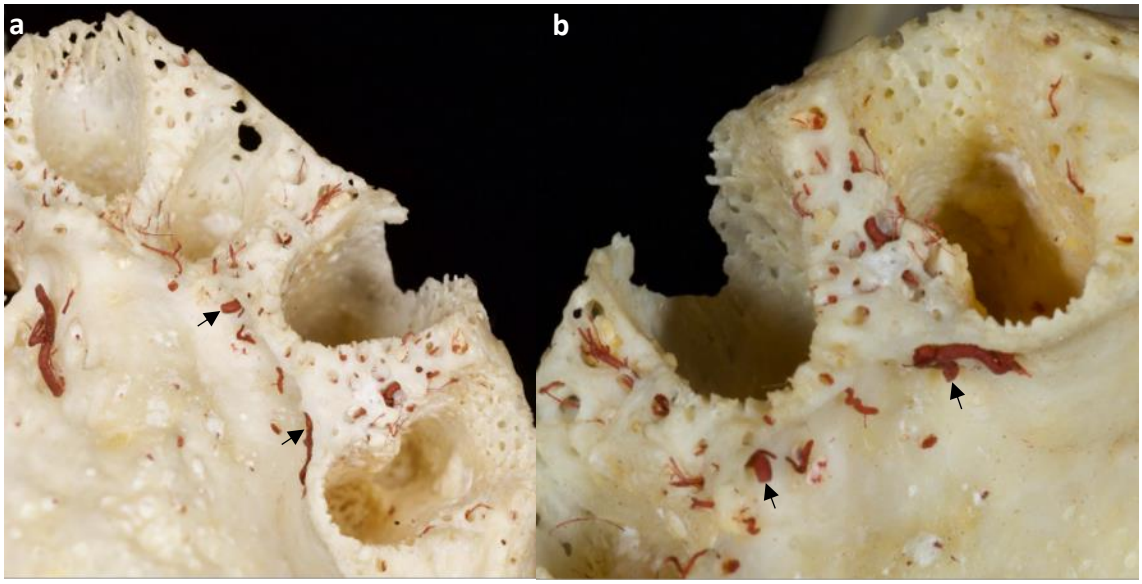

Fig. 4 Horizontal intraosseous anastomoses (transverse loop) **(a)** Overview of left front teeth after extraction, transalveolar anastomoses in the interdental septum marked with arrows. **(b)** Marked transverse loop; the intraosseous artery at the palatal aspect exhibits a larger dimension than the vestibular side, and small intraseptal branches are observed. (74)

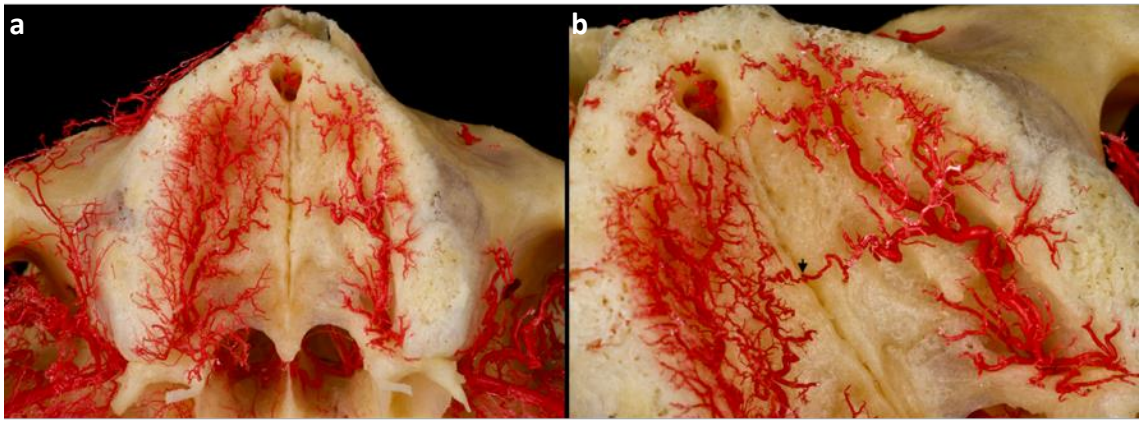

Fig. 5 Determination of penetrating intraosseous branch at the midpoint of the hard plate in the median palatine suture. **(a)** Overview of hard palate arterial supply with bilateral anastomosis between greater palatine arteries (GPAs). **(b)** A direct penetrating branch (↑) from bilateral anastomosis of GPAs entering median palatine suture. (166)

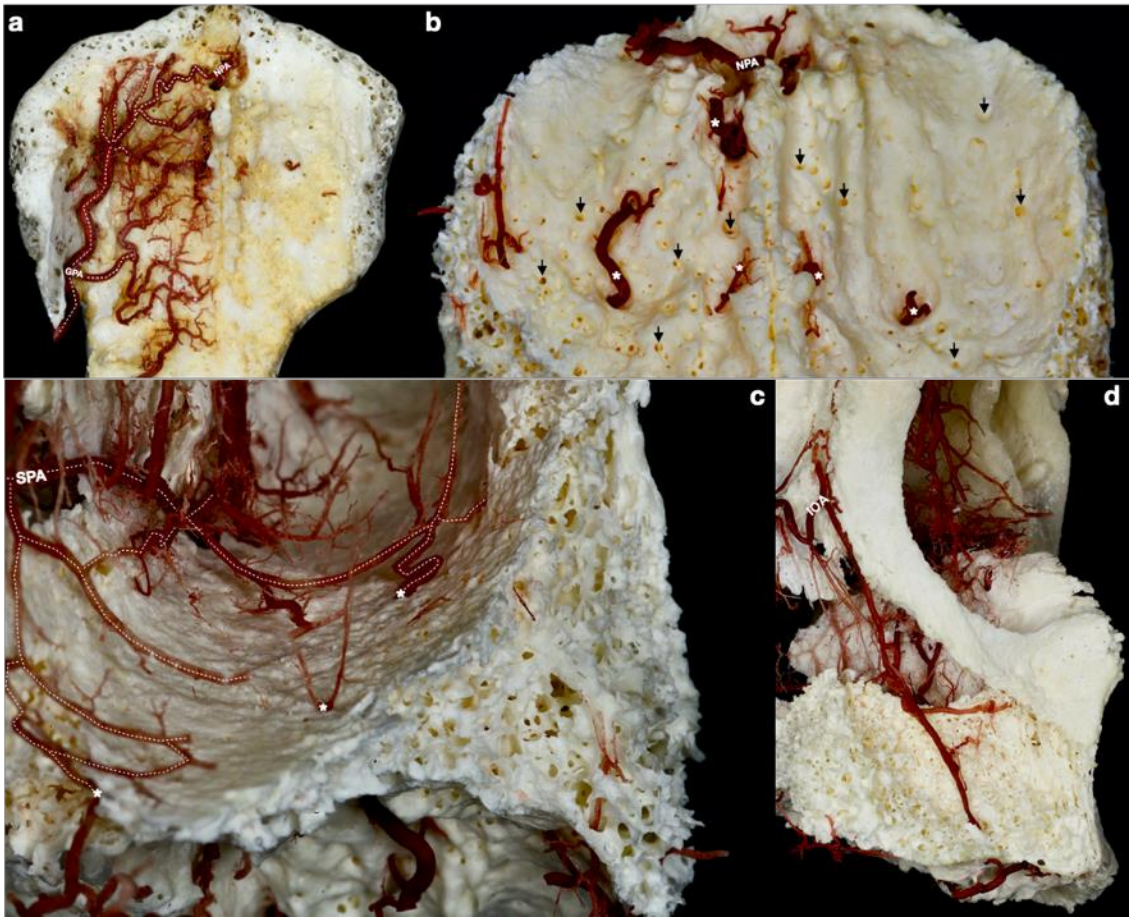

Fig. 6 Anastomoses pattern of the hard palate with the nasal cavity and maxilla. **(a)** Overview of extraosseous mapping of the greater palatine artery (GPA) branches with anastomosis to the nasopalatine artery (NPA). **(b)** After removing extraosseous branches of GPA osseous branches (*) are noticed in the anterior and middle aspects of the hard palate with several bony openings labeled with arrows (↓). **(c)** Posterior view from the floor of the nasal cavity, perforating branches (*) of GPA forming anastomoses with the branches of the posterior septal nasal branches of the sphenopalatine artery. **(d)** Anterolateral view of right maxilla, intraosseous branch of the infraorbital artery (IOA) supplies mainly the alveolar ridge territory, establishing collateral circulation between the maxilla and hard palate. (166)

4.2. Vascular architecture in the unilateral cleft palate

In the fetal specimen, the GPA was enlarged and orientated more laterally. (166) The extraosseous vessels were described according to their anastomosing patterns into a medial cleft zone and a lateral non-cleft zone related to the position of the GPA. The following observations were made (Fig. 7):

- In the cleft zone, the bilateral GPA anastomoses and, hence, palatal perforating and penetrating arteries were absent due to the cleft appearance. However, the GPA and its branches followed the non-cleft anatomy until the cleft edges limited them. The vessels did not follow the cleft borders but ran perpendicular to them.
- In the non-cleft zone, the branches of GPA were enlarged and anastomosed with subbranches of the FA/IOA in the anterior aspect of the palate. These anastomoses were found over the alveolar ridge. One GPA branch crossed the alveolar ridge in the anterior portion of the palate. The musculature of the soft palate attached from an anterolateral direction to the left GPA on the hard palate.

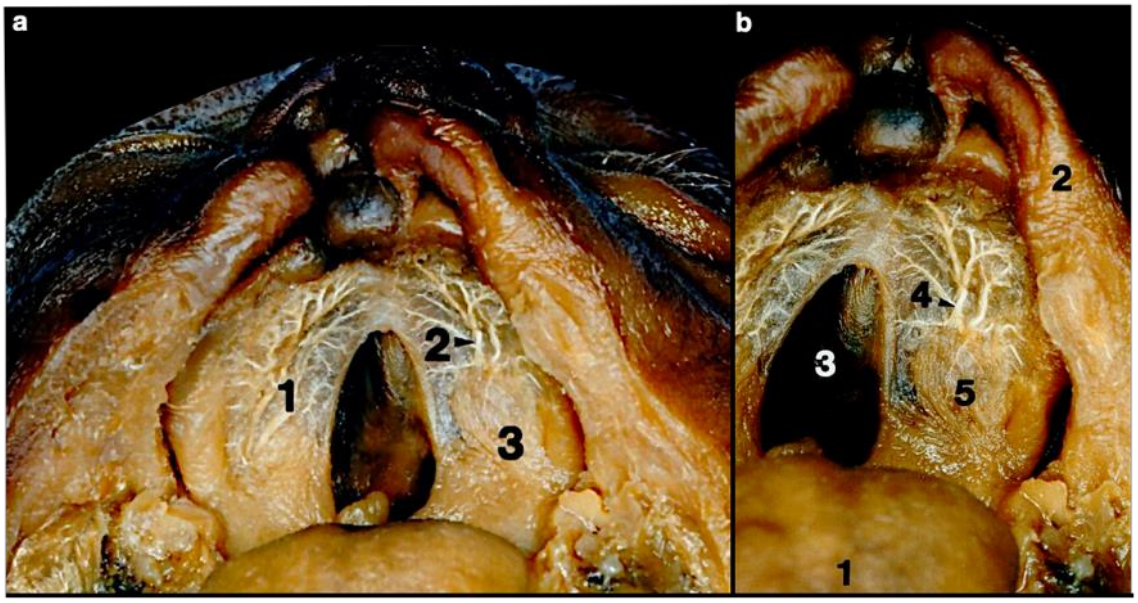

Fig. 7 Fetus with incomplete alveolar cleft with unilateral complete hard and soft palate cleft injected with barium sulfate. **(a)** Overview of the cleft palate, arterial distribution of the greater palatine artery (GPA) after mucosal dissection where contralateral anastomoses are omitted. 1- Hard palate; 2- GPA; 3- Fibres of soft palate muscle. **(b)** The allocation of GPA sub-branches in developed and unaffected areas, the vascularization in non-affected zones is maintained, particularly in the anterior palato-premaxillary territory. 1-Tongue; 2- Upper lip; 3- Cleft zone; 4- Non-cleft zone with GPA sub-branches; 5- Fibres of soft palate muscle. (166)

4.3. Upper lip musculovascular architecture influencing cleft lip-nose repair

4.3.1. Muscular organization

The myrtiform fossa was the origin of several muscles influencing nasolabial muscle vectors in the superficial and deep plane (Fig. 8). (58)

In the superficial plane three muscles were identified such as the LLSM, the LLSANM, and the incisivus labii superioris muscle (ILSM) which integrates into the OOM. No direct attachments to the lateral crus were identified from the aforementioned muscles; instead, connections were observed primarily through dense connective tissue extending into the deeper plane (Fig. 8).

In the deep plane of the myrtiform fossa, LLSM and LLSANM showed continuity by sending fibres to the deep muscles, again three muscles were observed from medial to lateral: the DSNM, the MM, and the nasalis (NM) muscles with alar (ANM) and TNM part. All three originated with periosteal attachments from the myrtiform fossa, ranging between the medial and lateral apex of the canine and first incisor (Fig. 8, 9). Together we labelled these muscles as the myrtiform muscular system (MMS), because of their intricate and interdependent functionalities, reflecting their cooperative dynamics within the nasolabial region. The TNM followed the contour of the nose and was inserted into the dorsum of the nose. The ANM connected to the lateral surface of the lateral alar crus and its fibrofatty tissue. The DSNM maintained a consistent anchorage to the cartilaginous nasal septum and the nasal tip from an inferior direction. Fibres of the ILSM originated from both the underlying DSNM and the myrtiform fossa.

The MMS showed two different patterns, based on the presence of the MM. A W-shaped pattern was observed in 69.2% and a V-shaped pattern was observed in 30.8% (Fig. 9).

The W-pattern was formed laterally by the NM, centrally by the fibres of the MM, and medially by the DSNM. The MM originated either from the myrtiform fossa or from the base of the DSNM.

Based on the cranial attachment of the MM, three distinct W-patterns were identified, each oriented toward the alar base, the nasal sill or both:

- Type Wa (55.5%): The MM attaches to the alar base (Fig. 9a).
- Type Wb (33.3%): The MM attaches to the nasal sill (Fig. 9b).
- Type Wc (11.1%): The MM splits into two heads, attaching to both the alar base and the nasal sill (Fig. 9c).

The V-pattern appeared when the MM was absent and was formed by the NM and DSNM, positioned laterally and medially, respectively, and replaced the absent MM (Fig. 9d). Either muscle could become dominant, though both were more developed in V-patterns compared to their appearances in W-patterns. In one specimen, a dominant NM extended its attachment 1.5 cm lateral to the alar base—esthetically resulting with wider nostrils.

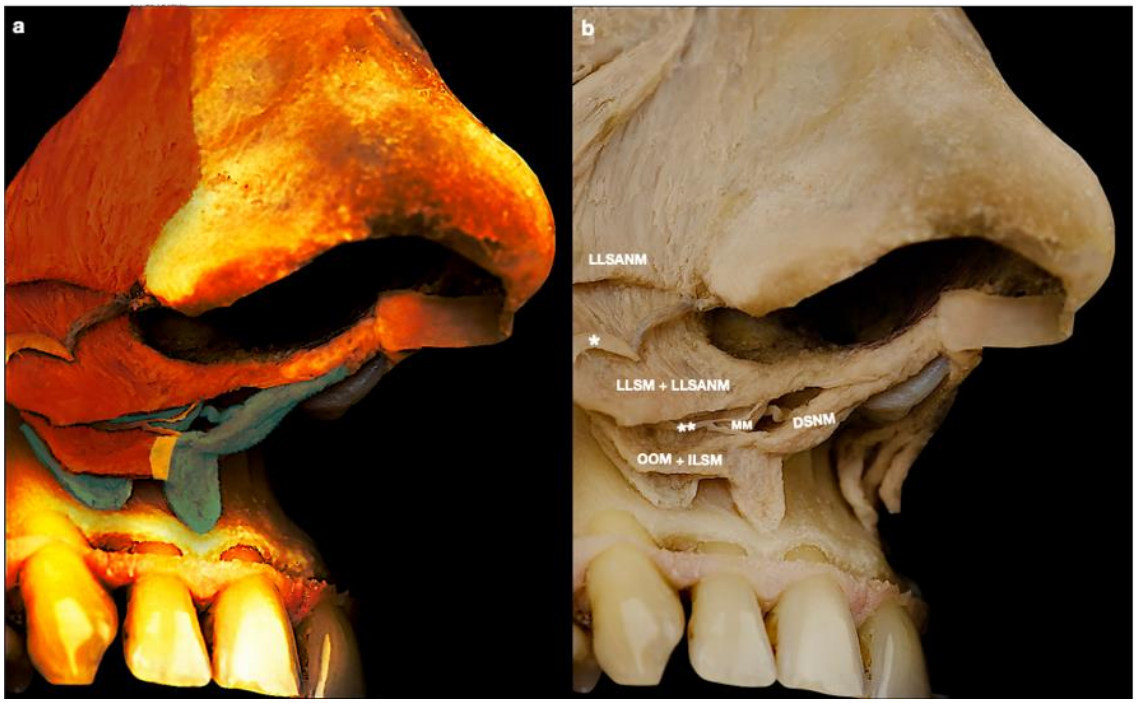

Fig. 8 Myrtiform area with the superficial and deep components of the myrtiform muscular system (MMS). **(a)** Illustration demonstrating the superficial (red) and deep (blue) components of the MMS. The two layers are interconnected by dense connective tissue (yellow), providing structural integration and functional continuity between the superficial and deep muscle fibres. **(b)** An anterolateral perspective of the different layers of muscles within the myrtiform fossa in a formalin-embalmed adult specimen. The levator labii superioris alaeque nasi muscle (LLSANM), the levator labii superioris muscle (LLSM), the orbicularis oris muscle (OOM) (majorly removed—extends across the entire myrtiform fossa), and the incisivus labii superioris muscle (ILSM) are situated in the superficial layer and connect to the dense connective tissue and muscles in the deep myrtiform fossa region. The branch of the facial artery (*) ascends above the superficially positioned muscles. Fibres originate from the myrtiform fossa and extend laterally to connect with the body of the OOM. The deep layer contains the depressor septi nasi muscle (DSNM), myrtiformis muscle (MM), and nasalis muscle. Branches of the infraorbital artery (**) traverse between the deep and superficial muscles. The nasalis muscle is covered by the LLSM and LLSANM. The myrtiform fossa is divided into two parts: the lateral part displays the origin of the nasalis muscle and the medial part indicates the origin of the DSNM. The intact nasal sill highlights the connection of the OOM and DSNM through dense connective tissue. (58)

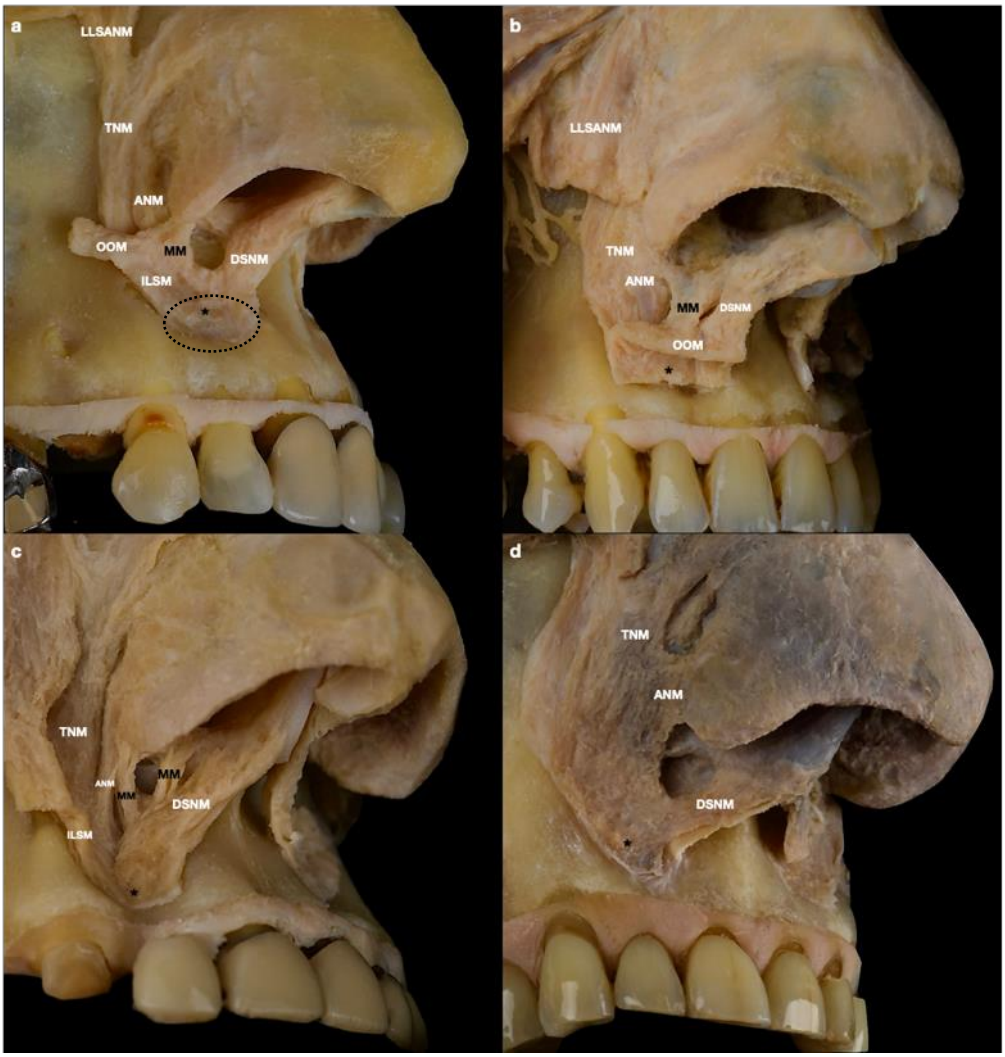

Fig. 9 Anterolateral aspect of the right myrtiform fossae and the nasal alae, highlighting several variations of the myrtiform muscular system (MMS) originating from the myrtiform fossa (dashed circle), in formalin-embalmed specimens. The transverse part of the nasalis muscle (TNM) is consistently positioned lateral to the alar part of the nasalis muscle (ANM). The nasalis muscle (NM) and depressor septi nasi muscle (DSNM) exhibit consistency. The existence and attachment of the myrtiformis muscles (MM) are variable. **(a)** Type Wa: The MM is connected to the alar base. The fibres of the incisivus labii superioris muscle (ILSM) integrate into the primary structure of the orbicularis oris muscle (OOM). **(b)** Type Wb: the MM is connected to the nasal sill. The levator labii superioris alaeque nasi muscle (LLSANM) is situated superior to both NM parts. **(c)** Type Wc: Two heads of MM extend toward the nasal sill and the alar base, forming a 'Y′-shaped configuration. The MM is connected to the DSNM. **(d)** Type V: The MMS is constructed by the DSNM and notable NM. The MM is principally missing. The periosteal origin of the MMS is more pronounced and attains the level of the nasal ala. *Myrtiform area with MMS connected through dense connective tissue. (58)

4.3.2. Vascular organization

Vascularization of the alar base, the nasal sill and the nasal septum was provided by branches of the FA, SLA, IOA, and dorsal nasal artery (DNA) with variable contributions. The extent of these contributions largely depended on the morphology and dominance of the SLA. A unilateral dominance was observed in 85% of cases with a tendency toward for right-sided SLA dominance (right/left = 60/40). The dominant side provided arterial supply not only to the ipsilateral-, but also to the contralateral lip, philtrum, and parts of the nostril area based on four subtypes:

- In type A (35.7%), the ipsilateral nostril region—including the ala and base, nasal sill, and septum—was supplied by the FAs and SLAs. The superior part of the ala received branches of the lateral nasal branch of the FA, while the subalar branch (SAB), arising directly from the FA, supplied the inferior part of the ala in the superficial plane. SLA sub-branches were identified in the deep plane. Although the SLA showed no dominant supply pattern, the philtral and septal branches (PSB) of SLA showed a unilateral dominancy and contributed to the supply of the contralateral nasal septum (Fig. 10a; Fig. 11).
- In type B (35.7%), a pronounced asymmetry with a unilateral dominant SLA. The dominant SLA supplied the ipsilateral nostril as well as the contralateral nasal septum. In this type the SAB originated from the SLA and SLA sub-branches to the contralateral nasal sill and alar base were observed. On the weak SLA side, the ala and the nasal sill were instead supplied by branches of the FA (Fig. 10b).
- In type C (21.4%), the asymmetry of the SLA was even more pronounced. On one side the FA/SLA was only rudimentary and did not contribute to the vascularization of the ala and nostril area. In contrast, the contralateral FA/SLA was dominant and followed the distribution patterns described in type A or type B. This dominant FA/SLA side supplied the contralateral nasal septum and nasal sill and additionally gave branches to the alar base. In two specimens, the dominant SLA ended as the contralateral angular artery. On the side where the FA/SLA was only rudimentary built, the IOA acted as a compensatory role, providing a more substantial contribution to the vascular supply of the region. As

a result, the supply of the deep portion of the alar base relied on the IOA. The IOA branches coursed from deep to superficial muscular planes, while FA branches penetrated from superficial to deep muscular planes and created several anastomoses. The pathways of these two vascular entities created multiple compensatory anastomoses (Fig. 10c).

- In type D (7%), the IOA and DNA (branch of the ophtalmic artery) supplied the ala on the weak SLA/FA side. Notably, both the IOA and DNA gave rise to lateral nasal branches which coursed through dense connective tissue to reach the internal aspect of the piriform aperture. SABs were derived predominantly from the IOA. The contralateral arterial distribution was consistent with the patterns described in previous types A–C (Fig. 10d).

Our findings revealed that the SABs of the FA were distributed superficially to the LLSANM, whereas the SLA coursed under the OOM and gave rise to several deep and superficial vertical and oblique PSBs. The deep branches pierced the OOM to reach the nostril surface. Constantly superficial and deep branches continued through the columella to the nasal tip. At this point they anastomosed with lateral nasal branches of the FA, the DNA and IOA branches, forming a dense vascular network around the nostrils.

Meanwhile, IOA branches coursed in a predictable manner under the LLSANM and superficial to the NM. The main IOA branch followed a medial path and the terminal artery perforated at the medial border of the LLSANM emerging to the surface and then accompanying the DSNM en route to the nasal septum. In multiple specimens, numerous IOA branches were observed to perforate the LLSANM, NM, or the MM before running on top of the periosteum.

Inside the floor of the nasal sill, two vascular arcades were detected. A superior arcade was composed by branches of either the FA or IOA, which followed the nostril rim from lateral to medial. The branches were situated superficially to the periosteum at the level of the piriform aperture and coursed deeply from the lateral alar cartilage to the medial cartilaginous septum. The inferior arcade, however, was mainly built by SLA branches. In specimens where the SLA was rudimentary, this inferior arcade exhibited variabilities in its configuration or was absent.

In addition, a dense band of connective tissue was observed linking the lateral nasal cartilages to the internal bone surface of the piriform aperture. This band was situated in the deepest layer of the lateral nostril and was supplied by mainly branches of the FA or IOA, depending on the above occurring type.

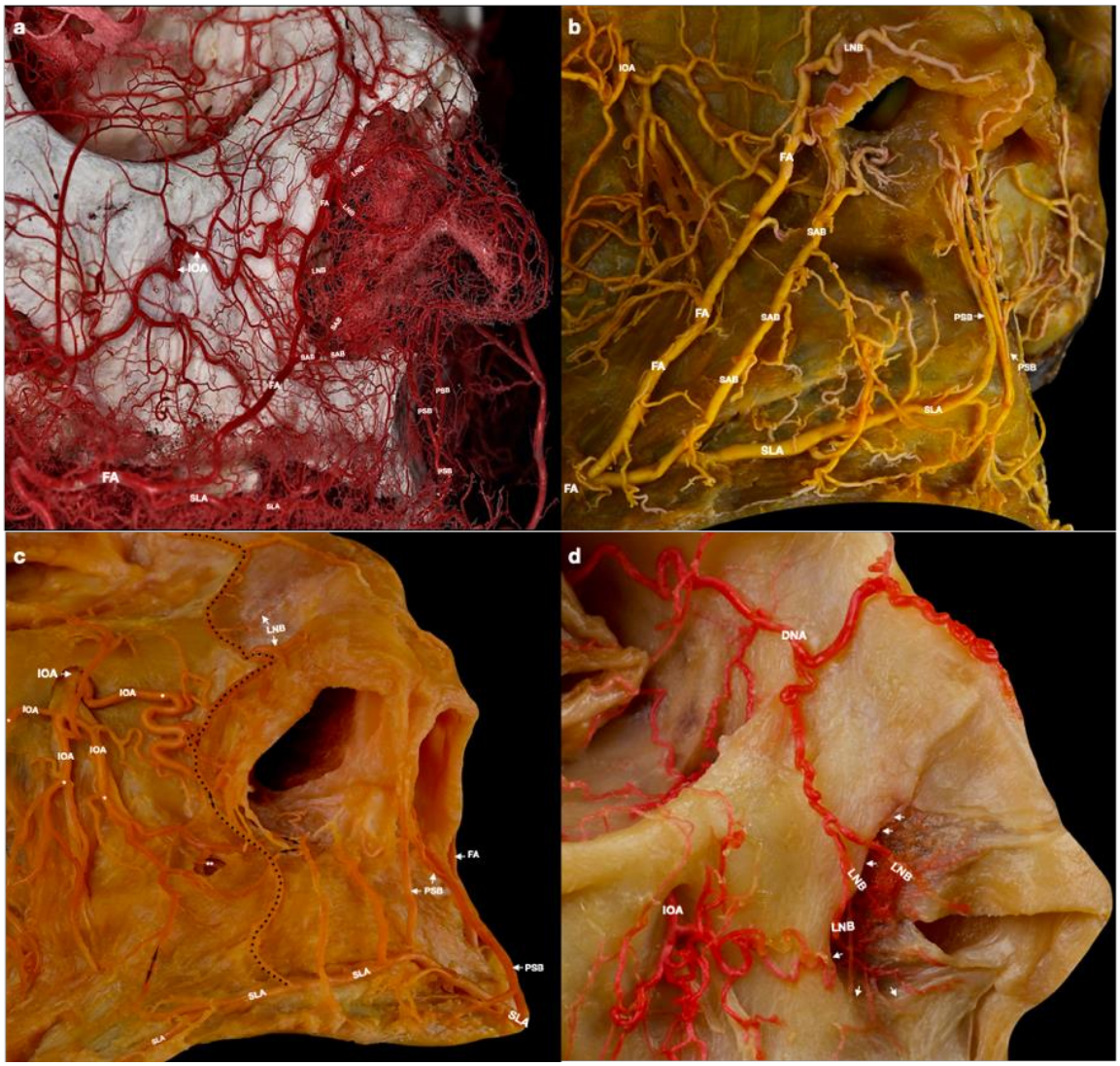

Fig. 10 Anterolateral view of the face with the subtypes of arterial division in the myrtiform area and lateral aspect of the nose. **(a)** Type A (corrosion casting, fresh/unfixed specimen), demonstrating the complexity of the superficial and deep arteries in the myrtiform area and lateral aspect of the nose forming several anastomoses. The subalar branch (SAB) derives from the facial artery (FA). Branches of the contralateral superior labial artery (SLA) supply the nasal septum dominantly. **(b)** Type B (specimen injected with latex and embalmed in Thiel), exhibiting a dominant SLA. The SAB diverges from the SLA and travels parallel to the FA until it perforates

the nasal sill, extending intranasally and laterally, with additional branches directed medially and laterally. The philtral septal branches (PSB) of the SLA and the lateral nasal branches (LNB) from the FA anastomose around the opening of the nose. **(c)** Type C (specimen injected with latex and embalmed in Thiel), demonstrating a rudimentary FA. The contralateral SLA (left side) supplies the nasal septum, ala, sill, and the lip together with the ipsilateral infraorbital artery (IOA). The IOA sends superficial (*) and deep branches (**). Crucial anastomoses between the IOA and the SLA at different levels are indicated by the black double-headed arrows. The IOA provides supply to the subalar region. Furthermore, the semicircular arcades are visible at the floor of the nasal sill. The contralateral SLA (left side) ends as the right side angular artery (black dotted line). **(d)** Type D (specimen injected with latex and embalmed in Thiel), showing the ala receiving its primary blood supply from the dorsal nasal artery (DNA) and the IOA. The lateral nasal branches (LNB) of the DNA and IOA specifically supply and infiltrate the connecting dense connective tissue linked to the internal aspect of the piriform aperture (white arrows). In this instance, the FA and SLA are not involved. (58)

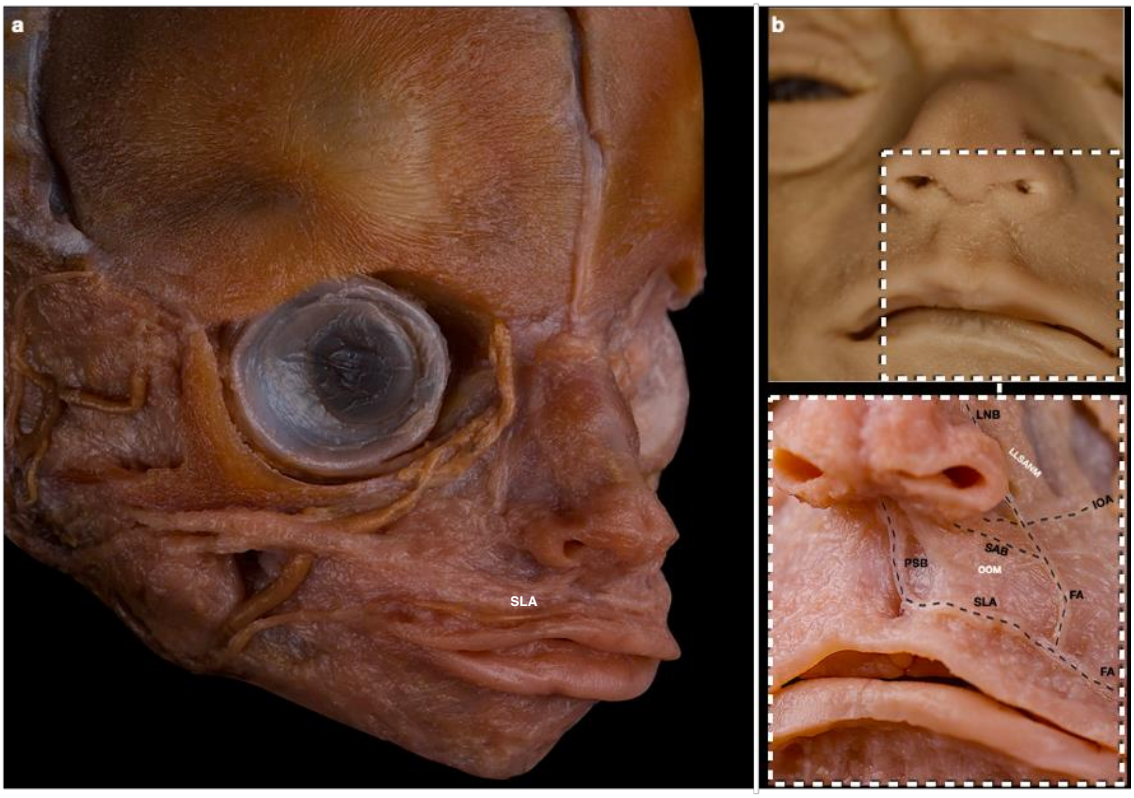

Fig. 11 Facial and nasolabial musculovascular anatomy of the 20- and 23-week gestational age formalin-fixed fetuses without vascular injection. **(a)** Overview of the anterolateral musculovascular aspect of the face, highlighting the superior labial artery (SLA). **(b)** Nasolabial area (upper) displaying musculovascular patterns (lower). The vascular mapping revealed the left-side-dominant SLA branching from the facial artery (FA) near the angle of the lips, with the philtral septal branch (PSB). The FA specifically provided the subalar branch (SAB) and continued as the lateral nasal branch (LNB). Anastomoses between the FA and the infraorbital artery (IOA) were identified in the lateral aspect of the ala, consistent with the results in the adults. OOM: orbicularis oris muscle (superficially dissected around the SLA to demonstrate its course); LLSANM: levator labii superioris alaeque nasi muscle. (58)

5. Discussion

The first reported cleft lip surgery dates back to the Chin Dynasty (119, 120). The surgeon, Fang Kan, cut the edges of a cleft lip and stitched them together. Over the centuries, various techniques and materials emerged until Franco pointed out the relation between cleft lip and cleft palate in the "Petit Traité" in 1556 (121). He released the soft tissues from the bony maxilla to allow approximation of the cleft edges. This concept laid the foundation for numerous techniques in the following decades and centuries. Many developments co-occurred at different European surgical schools, particularly in Germany and France, where access to anatomical cadaveric studies enhanced operative finesse and knowledge.

Based on this idea, in 1830, Dieffenbach performed extensive lateral releasing incisions intranasally and on the external skin to close wide clefts (122). Only 14 years later, Germanicus Mirault introduced a horizontal releasing incision (back-cut incision) above the white roll on the medial side of the cleft where a triangular flap from the lateral side was transposed (123). This technique influenced/formed the later Tennison-Randall Z-plasty, allowing the Cupid's bow preservation, which is a critical aesthetic aspect for upper lip harmony, but also allowing the closure of wide clefts (124–126). The mid-20th century was also characterized by significant contributions from Millard, who placed an arcuate incision beneath the columella allowing for an inferior rotational flap (127–129). This creates a skin muscle flap (rotation-advancement flap) which is attached in the opposed resulting gap. In a first step this flap design results in lip lengthening and favors the reconstruction of the nasal floor by rotating the nasal wing without disturbing the alar base (130, 131). However, the technique has also raised concerns about limiting further lip growth in the long term (132–135).

Other surgeons focused on a straight-line closure that dispenses with lateral releasing incisions—such as the French surgeon Victor Veau at the forefront, in the early 20th century (136). Although in the course of his career, with increasing experience, his straight-line closure aligned to a design similar to Mirault (123). Limberg later refined the straight closure design by integrating primary nasal correction and retaining a symmetrical Cupid's bow, which had been a challenge for Veau, along with other aesthetic impairments/considerations (123, 136, 137). Kilner adopted the conservative

straight-line closure with minimal tissue removal, drawing inspiration from techniques by Veau, Rose and Thompson (138).

Another concept mentioned by LeMesurier in 1935 is based on the functional repair alongside the closure of the cleft palate (139). The author highlighted the importance of not merely closing the defect but careful reconstructing the muscular and vascular anatomy to achieve successful speech and functional outcomes. This was expanded upon by Schilli (140) and later, Fara (141) advanced the technique introduced by Kilner by prioritizing anatomical restoration and precise reapproximation of the OOM fibres, which are transversally (142, 143) orientated towards the edges of the cleft. However, restoring OOM function alone did not resolve abnormal skeletal development. Delaire recognized that reconstruction must address the nasolabial musculature, comprising the perioral but also the paranasal musculature (144, 145). Furthermore, he demonstrated the insertion of the facial musculature onto the nasal septum rather than into the adjacent alar skin, which was later confirmed by magnetic resonance imaging (MRI) (144, 146).

The cleft disrupts the interaction between the primary and secondary facial growth centers, thereby affecting midfacial skeletal development. Joos therefore emphasized the need to restore the muscle-periosteum apparatus up to the zygomatico-maxillary suture to allow normal physiological growth between both facial growth centers (147). He compared skeletal development following two surgical approaches (group 1: restoration of the perioral, paranasal and muscle-periosteum apparatus reconstruction; group 2: OOM reconstruction in conjunction with orthopedic growth stimulation). Only 20% of patients in group 1 developed a Class III malocclusion, whereas 80% of patients in group 2 exhibited a Class III with marked maxillary and midface hyoplasia (147). These findings underscore that muscular reconstruction requires more than OOM repair alone and demand attention to deeper anatomical structures. Dentofacial orthopedic or orthodontic treatment cannot compensate for deficient skeletal growth resulting from inadequate surgery (147).

As demonstrated by our results, not only the OOM plays a role in restoring the cleft lip but also the nasolabial muscles (148) that influence the superficial musculoaponeurotic system (SMAS) (149, 150). We have focused on the muscles in the deep plane, forming together the MMS. A muscle system that consists of the interaction of the NM, the MM and the DSNM. All these muscles originate from the myrtiform fossa.

Our dissections reveal that the MMS consistently exhibits variable morphologies, influenced by the occurrence of the MM. This results in a vertically oriented W- or V-shaped MMS, constituting the deep layer of the modiolus alae nasi, and resemble to type 3 and type 2 as described by Uzmansel and Öztürk, respectively (36). With attachments to the lateral alar crus, depression and expansion of the nostrils can be executed. This effectively counterbalances the uplifting and narrowing effect of the superficial muscles, which are connected indirectly via the SMAS to the MMS, while lacking direct attachments to the alar cartilages. Hur et al. observed interconnections between the LLSANM and TNM in 90% of cases (151), which demonstrate the linkage of the MMS with adjacent muscles and dense connective tissue, thereby promoting force transmission onto the SMAS (149, 150).

The force vectors of the muscles are altered by the cleft, resulting in a deviation of the nasal septum to the non-cleft side. This effect is observable in the lateral nasolabial subunit of the cleft, where the lip, cheek, and nasal sill and nostril appear planar and the natural alar-facial groove is absent. Common operating techniques do not pay attention to the nasolabial muscles, which are very easily overlooked without prior anatomical knowledge, and detach their fibres. The nasolabial region can be described as two interlinked muscle slings (Fig. 12):

- Superficial Oral sling: Rounded like the letter "*o"* and encircles the mouth.
- Deep Nasal sling: Curved like the letter "*n"* and bridges the bilateral nasalis muscles across the nasal dorsum, forming an arch.

Both slings complete the appearance of a figure of "8" (152–154). However, in the presence of a cleft, the continuity of the oral sling is disrupted. This not only compromises the integrity of the figure "8" but also displaces the nasal sling, which causes the nasal arch to shift out of place (58) (Fig. 12).

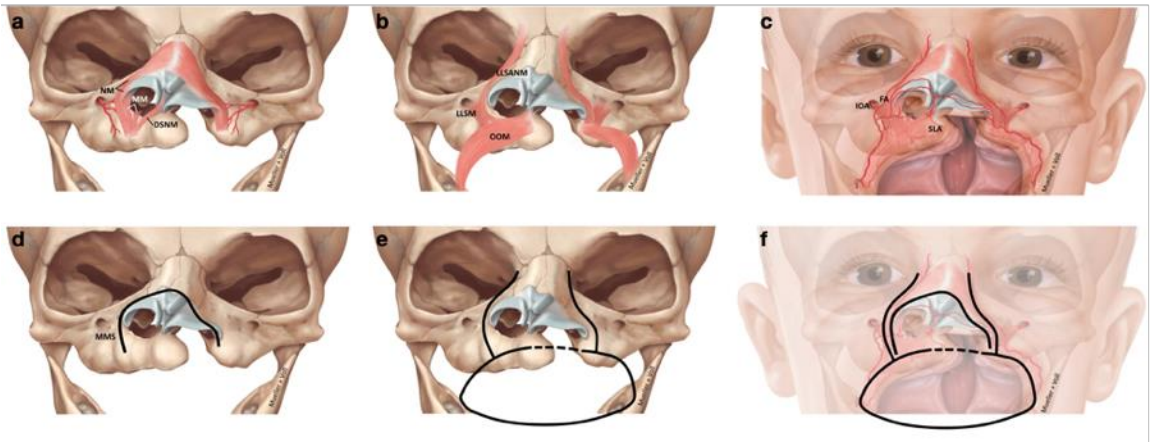

Fig. 12 Anterior view of an infant with unilateral complete cleft lip and palate, illustrating the superficial and deep nasolabial muscles in relation to the regional vessels. **(a)** The myrtiform muscular system (MMS) represents the deep nasolabial muscle layer comprising, from medial to lateral, the depressor septi nasi (DSNM), myrtiformis muscle (MM), and nasalis muscle (NM), along with the branches of the infraorbital artery (IOA), which partially perforate the MMS. **(b)** The superficial nasolabial musculature comprises the levator labii superioris (LLSM), levator labii superioris alaeque nasi (LLSANM), and orbicularis oris (OOM) muscles. **(c)** Facial artery (FA) branches run over the superficial muscles. The superior labial artery (SLA) predominantly courses beneath or between OOM fibres. **(d)** Simplified course of the MMS, representing the deep "n"-shaped nasal muscle sling connecting both myrtiform fossae. **(e)** Simplified trajectory of the superficial muscles with the oral "o" muscle ring being interrupted by the cleft (dashed line). **(f)** The composite view illustrates both the deep nasal "n" configuration and the superficial oral "o", resulting in the illusive nasolabial "8" double sling configuration. (58)

Detaching or dissecting single nasolabial muscles at the region of the alar base creates an empty triangle and alters the integrity of the SMAS, which in return makes it difficult to restore the missing alar-facial groove in cleft patients (155). To address this, we suggest detaching the MMS at its periosteal origin within the myrtiform fossa and transposing it to the periosteum of the vestibular sulcus on the non-cleft side, as similarly described by Talmant (156, 157). This maneuver restores the alar-facial groove from a planar position back to a physiological and symmetrical appearance by pulling the MMS mediocaudally (Fig. 13).

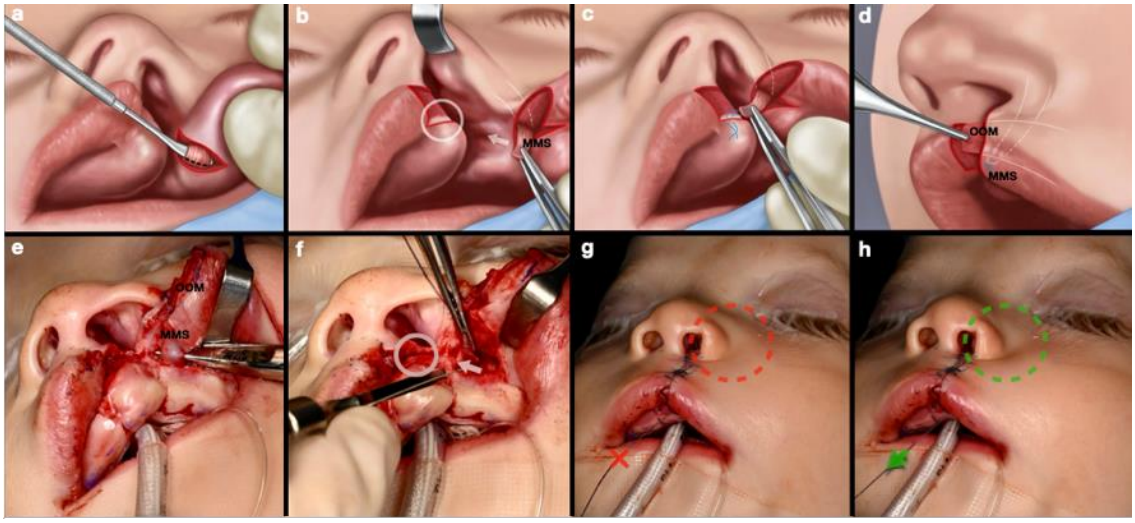

Fig. 13 Surgical steps in cleft lip-nose repair highlighting the muscular relationship between the myrtiform muscular system (MMS) and the orbicularis oris muscle (OOM). **(a, e)** Schematic illustration and surgical identification and release of the MMS from the cleft alveolar process. **(b, f)** Partial dissection and transposition to a new insertion on the premaxilla lateral to the incisor region. **(c)** Fixation of the MMS to the periosteum using sutures. **(d)** Crossover of the deep vertical MMS vector and superficial horizontal OOM vector. **(g, h)** Transformation of the alar-facial junction from a planar to a groove shape through suture-induced tension on the MMS, with final stabilization achieved by knot tightening. (58)

The MMS is consistently found at the mucogingival junction at the cleft border on the cleft side. Joos used a muscle stimulator during his dissection to identify the paranasal musculature, as he used to describe the MMS (158). Superficially, the restored OOM overlaps the transposed MMS. Repair of the OOM itself can be performed in two layers: the deep layer is sutured to its contralateral counterpart, whereas the superficial layer can be sutured lateral to the philtrum to create a philtral column (156). Readaptation of these dual muscular planes—the vertical MMS and horizontal OOM—reestablishes the figure of "8" configuration. In the case of wide clefts, the further advancement of the nasal ala is facilitated by the dissection of the alar-piriform aperture ligament. The ligament consists of dense connective tissue fibres which attaches to the internal aspect of the piriform aperture. In order to avoid MMS injury, its surgical access can be gained medially of the myrtiform fossa.

The DSNM, as part of the MMS, is not a reliable landmark on the cleft side, since it is missing or malpositioned. The uniform pull on the nasal septum by the contralateral DSNM results in the deviation toward the non-cleft side. On the cleft side, the DSNM fibres may course together with the NM fibres to ala on the cleft side, which could further contribute to nostril collapse.

It has been assumed that bone regeneration and development are ensured by maintaining the bone-periosteum connection intact, leading to the use of an epiperiosteal preparation (159). However, the epiperiosteal approach damages the periosteum, since its vascular supply originates from the soft tissues, underscoring the importance of keeping the soft tissue-periosteum connection intact and to favor a subperiosteal approach (147, 160, 161). Using the above-mentioned approach, it is advisable to isolate the MMS prior to subperiosteal mobilization, as this step renders its identification more difficult. Additionally, epiperiosteal preparation or dissection increases the risk of relevant vessel injury in the nasolabial area, such as the IOA, FA, SAB and SLA. In our dissections we could also detect the DNA, which is a branch of the ophthalmic artery, contributing to the vascular supply of the nasal ala, when the FA is rudimentary. We observed the unilateral dominancy of the SLA in the vascularization of the upper lip without cleft. A phenomenon which was earlier encountered by Lee et al. (55) in the upper lip with contralateral nasal septum supply in 15% and by Ricbourg in the lower lip.

Ricbourg furthermore noticed cases with no anastomosis between right and left SLA in the upper lip with various collateral arteries supplying the nasal septum, the philtrum and the nostril base (162). This follows the principles of Salmon and Mitz et al. who described the counterbalancing effect of a weak artery by the hypertrophy of a neighboring artery to cover the supply (163, 164).

This may play a critical role when considering its relevance in cleft anatomy. A cleft relies on fewer vascular supply anastomoses compared to non-cleft anatomy. Preserving these vessels will greatly contribute to the healing quality and the success of the surgery (151, 165). Therefore, dissection of individual muscles or sharp preparations should be exercised with caution due to the pathway of the IOA overlying the MMS. In contrast, the area beneath to the MMS delineates a safer zone with less larger vessels. In addition, the IOA courses with intraosseous vessels along the anterior maxillary wall, forming anastomoses with its contralateral counterpart within the anterior nasal spine (166) (Fig

2). The anterior nasal spine is part of the premaxilla, with distinct relevant anastomoses between the IOA-GPA-NPA-SPA, forming an intraosseous anastomosing network supplying the anterior alveolar process and anterior palate, which is, however, partially disrupted in the presence of a cleft (74, 167, 168).

In the case of a cleft of the hard palate, the anastomosis and compensation effect of the bilateral GPA anastomosis, from which penetrating branches may arise, is absent (70, 166). The palatal vascularization becomes more dependent on collateral intra- and extraosseous blood flow, especially in the event of GPA or descending palatine artery injury; therefore, incisions must be chosen carefully (169). Otherwise, fistula occurrence or avascular necrosis may occur (165, 170–172). In unilateral clefts, an NPA-GPA anastomosis is present on the non-cleft side (Fig. 7); however, in bilateral clefts, no NPA-GPA anastomosis can be observed. The flap design needs to be adapted to its absence.

The developmental vascularization of the palate is supported by branches of the FA traversing the alveolar ridge (173). Von Langenbeck introduced the elevation of bilateral bipedicled mucoperiosteal flaps to close the cleft by performing bilateral incisions along the cleft margins (174). In combination with the traditional bilateral releasing incisions—placed lateral to the GPA on the palatal mucoperiosteum and extending from the tuberosity toward the anterior alveolar ridge without anterior unification—approximation in the midline was possible. Notably, collateral vascularization in the anterior and posterior aspects is preserved, in contrast to the disrupted collateral system along the lateral aspect (Fig. 14b). Delaire et al. and Markus et al. introduced modifications of the Von Langenbeck technique by placing the bilateral releasing incisions medial to the GPA (175–177). From a vascular perspective, this disrupts the perpendicular blood flow from the GPA to the cleft margins and narrows the supply of anterior and posterior collaterals.

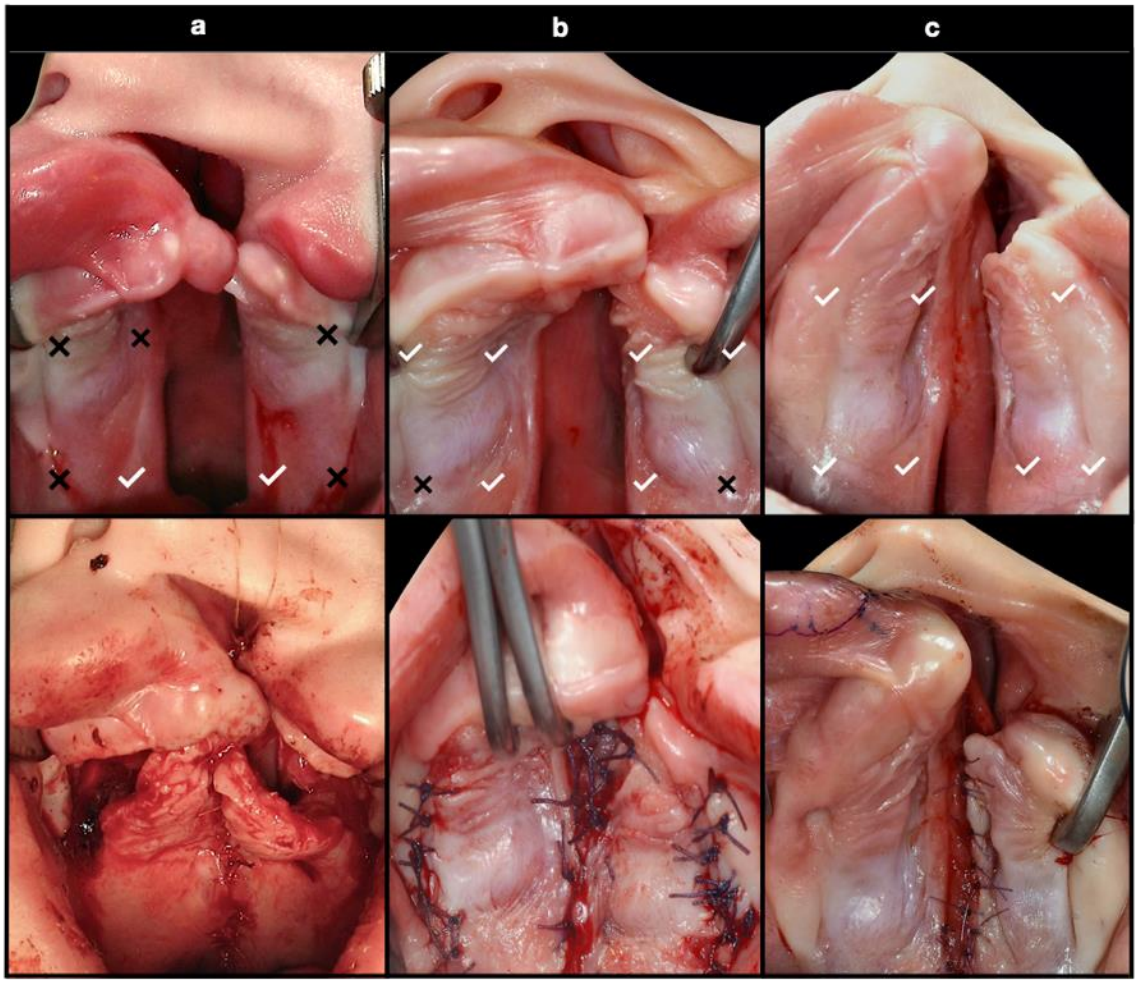

Fig. 14 Comparative change of vascular collateral supply in various techniques of palate cleft surgery (preoperative (above) and postoperative (below) aspects of each patient). Collateral zones are labeled as affected (×) or preserved (✓) at critical regions: Anterolateral GPA-IOA-FA, Anteromedial GPA-NPA, Posterolateral GPA-LPA-PSAA-MA, Posteromedial GPA-LPA-APA-APHA. **(a)** Uni-pedicle flap. **(b)** Bi-pedicle flap. **(c)** Minimal incision palatoplasty (combined with continuous circular closure). Greater palatine artery (GPA); Infraorbital artery (IOA); Facial artery (FA); Nasopalatine artery (NPA); Lesser palatine artery (LPA); Posterior superior alveolar artery (PSAA); Maxillary artery (MA); Ascending palatine artery (APA); Ascending pharyngeal artery (APHA). (166)

At the junction of the hard and soft palate, in the posterior aspect, the soft palate arteries—including the LPA, ascending pharyngeal, and ascending palatine arteries—provide an important vascular supply, while the maxillary artery may course in close proximity to

the maxillary tuberosity (166, 169) (Fig. 1, 14). This becomes relevant when closing the hard palate cleft after Veau (83). Veau connected the bilateral incisions in the anterior palate with the incisions at the cleft margins to allow the elevation of two unipedicled flaps, relying solely on GPA and the soft palate. Several modifications based on this approach have been published (178–181). However, from a vascular perspective, the collateral supply is further constricted. This contrasts to the beginnings of cleft hard palate closure in 1826, where Dieffenbach performed simple mucosal elevation and suturing (182). Minimal invasive incision designs continue to be employed today (172), however in wide palatal clefts, releasing incisions become indispensable to achieve closure, necessitating a transition from a minimal invasive design to bipedicled or even unipedicled flaps (183) (Fig. 14a, b).

6. Conclusions

Successful cleft surgery is fundamentally dependent on precise morphological understanding to achieve optimal functional and aesthetic outcomes while minimizing complications.

In the hard palate/alveolar studies, various intra- and extraosseous collateral networks were identified in normal adult palates. However, in the hard palate cleft fetus, the GPA appeared enlarged and laterally displaced, forming alternative anastomotic patterns. The findings indicated that, although vascular continuity was reduced within the cleft zone, arterial configurations in the non-cleft regions largely preserved normal circulation, with maintained anastomotic networks. In contrast, the reduced microcirculation within the cleft area underscored the critical importance of preserving existing vascular pathways—particularly in the regions of the incisive canal, alveolar ridges, and retrotuberal area—to ensure adequate perfusion.

In the myrtiform area study, the MMS demonstrated a W- or V-shaped configuration with considerable vascular variability, characterized by unilateral dominance of the SLA and compensatory contributions from adjacent arterial systems. Vascular mapping further identified four distinct patterns (types A–D), reflecting significant variation in arterial supply to the lip and alar region. Intraoperative observations revealed that, although muscular attachments resembled normal anatomy, cleft-related displacement led to distortion of muscular vector orientation. These findings clarified the musculovascular morphology in relation to the surgical intervention and demonstrated that restoration of a natural alar-facial groove in cleft lip-nose repair could be achieved by detaching and repositioning the origin of the MMS. This approach corrected cleft-induced muscular vector distortion while preserving the anatomical insertion at the alar base, allowing realignment without extensive dissection.

Overall, these results highlight the importance of adapting surgical techniques to the underlying vascular and muscular anatomy. Preservation of critical anastomotic pathways and careful consideration of muscle vector orientation are essential for maintaining tissue perfusion, thereby enhancing wound healing and reducing complications in cleft repair.

7. Summary

This dissertation investigated the vascular collateral networks of the hard palate and the musculovascular architecture of the nasolabial region, with direct relevance to cleft and reconstructive surgery. Given the global prevalence of cleft lip and palate, a detailed anatomical understanding is essential for optimizing surgical outcomes. Our studies provided a comprehensive morphological analysis of vascular and muscular patterns with direct clinical relevance for cleft repair.

By utilizing advanced anatomical techniques—including embalming methods, latex injection, and corrosion casting—both intra- and extraosseous vascular pathways of the hard palate and alveolar aspects, as well as the musculovascular patterns of the upper lip, were delineated and investigated.

In the normal hard palate and alveolar regions, extensive intra- and extraosseous collateral networks were identified, supporting robust collateral perfusion. In contrast, the cleft specimen demonstrated altered vascular patterns, including enlargement and lateral displacement of the GPA, absence of key anastomoses within the cleft zone, and more perpendicular orientation of arterial branches toward the cleft margins, thereby emphasizing the need for preservation of the dominant vascular supply during surgical intervention.

In the study of the myrtiform area, the MMS was defined as a consistent anatomical entity with W- or V-shaped configurations and significant vascular variability, characterized by unilateral dominance of the SLA and compensatory contributions from adjacent arterial systems. The findings highlighted the importance of recognizing musculovascular organization and compensatory perfusion patterns in clef lip-nose repair.

Based on our determinations a comprehensive anatomical foundation for a more anatomically guided approach in cleft surgery. The findings emphasize that surgical planning should be tailored to the underlying musculovascular architecture, with particular attention to preserving key vascular pathways and respecting muscle orientation. Such an approach may contribute to improved tissue viability, enhanced wound healing, and more predictable functional and aesthetic outcomes in cleft repair.

8. References

1) Arnold F, West DC. Angiogenesis in wound healing. Pharmacol Ther. 1991;52(3):407-22.

2) Zhang Z, Fang S, Zhang Q, Chen L, Liu Y, Li K, Zhao Y. Analysis of complications in primary cleft lip and palates surgery. J Craniofac Surg. 2014;25(3):968-71.

3) Ren S, Ma L, Sun Z, Qian J. Relationship between palate-vomer development and maxillary growth in submucous cleft palate patients. Cleft Palate Craniofac J. 2014;51(3):314-9.

4) Krogman WM, Jain RB, Oka SW. Craniofacial growth in different cleft types from one month to ten years. Cleft Palate J. 1982;19(3):206-11.

5) Katzel EB, Basile P, Koltz PF, Marcus JR, Girotto JA. Current surgical practices in cleft care: cleft palate repair techniques and postoperative care. Plast Reconstr Surg. 2009;124(3):899-906.

6) Murthy J. Complications of cleft palate repair and how to avoid them. J Cleft Lip Palate Craniofac Anomal. 2014;1(1):19-25.

7) Deshpande GS, Campbell A, Jagtap R, Restrepo C, Dobie H, Keenan HT, Sarma H. Early complications after cleft palate repair: a multivariate statistical analysis of 709 patients. J Craniofac Surg. 2014;25(5):1614-8.

8) Mossey PA, Little J, Munger RG, Dixon MJ, Shaw WC. Cleft lip and palate. Lancet. 2009;374(9703):1773-85.

9) Carroll K, Mossey PA. Anatomical variations in clefts of the lip with or without cleft palate. Plast Surg Int. 2012;2012:542078.

10) Panamonta V, Pradubwong S, Panamonta M, Chowchuen B. Global birth prevalence of orofacial clefts: a systematic review. J Med Assoc Thai. 2015;98(Suppl 7):11-21.

11) Salari N, Darvishi N, Heydari M, Bokaee S, Darvishi F, Mohammadi M. Global prevalence of cleft palate, cleft lip and cleft palate and lip: A comprehensive systematic review and meta-analysis. J Stomatol Oral Maxillofac Surg. 2022;123(2):110-20.

12) Inchingolo AM, Fatone MC, Malcangi G, Avantario P, Piras F, Patano A, Di Pede C, Netti A, Ciocia AM, De Ruvo E, Viapiano F, Palmieri G, Campanelli M, Mancini A, Settanni V, Carpentiere V, Marinelli G, Latini G, Rapone B, Tartaglia GM, Bordea IR,

Scarano A, Lorusso F, Di Venere D, Inchingolo F, Inchingolo AD, Dipalma G. Modifiable Risk Factors of Non-Syndromic Orofacial Clefts: A Systematic Review. Children. 2022;9(12):1846.

13) Askarian S, Gholami M, Khalili-Tanha G, Tehrani NC, Joudi M, Khazaei M, Ferns GA, Hassanian SM, Avan A, Joodi M. The genetic factors contributing to the risk of cleft lip–cleft palate and their clinical utility. Oral Maxillofac Surg. 2023;27(2):177-86.

14) Avasthi KK, Muthuswamy S, Asim A, Agarwal A, Agarwal S. Identification of novel genomic variations in susceptibility to nonsyndromic cleft lip and palate patients. Pediatr Rep. 2021;13(4):650-7.

15) Amooee A, Dastgheib SA, Niktabar SM, Noorishadkam M, Lookzadeh MH, Mirjalili SR, Heiranizadeh N, Neamatzadeh H. Association of fetal MTHFR 677C>T polymorphism with non-syndromic cleft lip with or without palate risk: a systematic review and meta-analysis. Fetal Pediatr Pathol. 2021;40(4):337-53.

16) Ludwig KU, Böhmer AC, Rubini M, Mossey PA, Herms S, Nowak S, Reutter H, Alblas MA, Lippke B, Barth S, Paredes-Zenteno M, Muñoz-Jimenez SG, Ortiz-Lopez R, Kreusch T, Hemprich A, Martini M, Braumann B, Jäger A, Pötzsch B, Molloy A, Peterlin B, Hoffmann P, Nöthen MM, Rojas-Martinez A, Knapp M, Steegers-Theunissen RP, Mangold E. Strong association of variants around FOXE1 and orofacial clefting. J Dent Res. 2014;93(4):376-81.

17) Dai J, Xu C, Wang G, Liang Y, Wan T, Zhang Y, Xu X, Yu L, Che Z, Han Q, Wu D, Yang Y. Novel TBX22 mutations in Chinese nonsyndromic cleft lip/palate families. J Genet. 2018;97(2):411-7.

18) Xu M, Ma L, Lou S, Du Y, Yin X, Zhang C, Fan L, Wang H, Wang Z, Zhang W, Wang L, Pan Y. Genetic variants of microRNA processing genes and risk of non-syndromic orofacial clefts. Oral Dis. 2018;24(3):422-8.

19) Yoneda T, Pratt RM. Vitamin B6 reduces cortisone-induced cleft palate in the mouse. Teratology. 1982;26(3):255-8.

20) DeRoo LA, Wilcox AJ, Lie RT, Romitti PA, Pedersen DA, Munger RG, Moreno Uribe LM, Wehby GL. Maternal alcohol binge-drinking in the first trimester and the risk of orofacial clefts in offspring: a large population-based pooling study. Eur J Epidemiol. 2016;31(10):1021-34.

21) Scheller K, Röckl T, Scheller C, Schubert J. Lower concentrations of B-vitamin subgroups in the serum and amniotic fluid correlate to cleft lip and palate appearance in the offspring of A/WySn mice. J Oral Maxillofac Surg. 2013;71(9):1601.e1-7.

22) Ishii LE, Byrne PJ. Lip reconstruction. Facial Plast Surg Clin North Am. 2009;17(3):445-53.

23) Nicolau PJ. The orbicularis oris muscle: a functional approach to its repair in cleft lip. Br J Plast Surg. 1983;36(2):141-53.

24) Wu J, Yin N. Detailed anatomy of the nasolabial muscle in human fetuses as determined by micro-CT combined with iodine staining. Ann Plast Surg. 2016;76(1):111-6.

25) Pepper JP, Baker SR. Local flaps: cheek and lip reconstruction. JAMA Facial Plast Surg. 2013;15(5):374-82.

26) Song R, Ma H, Pan F. The “levator septi nasi muscle” and its clinical significance. Plast Reconstr Surg. 2002;109:1707-12; discussion 1713.

27) Youn KH, Park JT, Park DS, Koh KS, Kim HJ, Paik DJ. Morphology of the zygomaticus minor and its relationship with the orbicularis oculi muscle. J Craniofac Surg. 2012;23(2):546-8.

28) Galyon SW, Frodel JL. Lip and perioral defects. Otolaryngol Clin North Am. 2001;34(3):647-66.

29) Briedis J, Jackson IT. The anatomy of the philtrum: observations made on dissections in the normal lip. Br J Plast Surg. 1981;34(2):128-32.

30) Latham RA, Deaton TG. The structural basis of the philtrum and the contour of the vermilion border: a study of the musculature of the upper lip. J Anat. 1976;121:151-60.

31) Tan O, Atik B. Triangular with Ala nasi (TAN) repair of unilateral cleft lips: a personal technique and early outcomes. J Craniofac Surg. 2007;18(1):186-97.

32) Shang J, Feng X, Chen Y, Gu Z, Liu Y. Human lip vermilion: physiology and age-related changes. J Cosmet Dermatol. 2024;23(8):2676-80.

33) Sappey PC. Traité d’anatomie descriptive. Tome 2. 3rd ed. Paris: A. Delahaye; 1876. p. 135-42.

34) Yeği NME, Bilge O, Çelik S. The myrtiformis muscle: identification of a forgotten entity that is distinct from the depressor septi nasi muscle. Cureus. 2023;15(3):e36214.

35) de Souza Pinto EB. Relationship between tip nasal muscles and the short upper lip. Aesthetic Plast Surg. 2003;27(5):381-7.

36) Uzmansel D, Öztürk NC. Revisiting the anatomy of myrtiformis muscle. Surg Radiol Anat. 2023;45(7):789-94.

37) Figallo EE, Acosta JA. Nose muscular dynamics: the tip trigonum. Plast Reconstr Surg. 2001;108(5):1118-26.

38) Rohrich RJ, Huynh B, Muzaffar AR, Adams WP Jr, Robinson JB Jr. Importance of the depressor septi nasi muscle in rhinoplasty: anatomic study and clinical application. Plast Reconstr Surg. 2000;105(1):376-83.

39) Aiach G. Atlas de rhinoplastie et de la voie d'abord externe. Paris: Masson; 1993. 216 p.

40) Brusati R, Mannucci N, Mommaerts MY. The Delaire Philosophy of Cleft Lip and Palate Repair. In: Waard-Booth P, Schendel S, Hausamen JE, editors. Maxillofacial Surgery. 2nd ed. Edinburgh: Churchill Livingstone; 2006. Ch. 52.

41) Hoeyberghs JL, Desta K, Matthews RN. The lost muscles of the nose. Aesthetic Plast Surg. 1996;20(2):165-9.

42) Daniel RK, Glasz T, Molnar G, Palhazi P, Saban Y, Journel B. The lower nasal base: an anatomical study. Aesthetic Surg J. 2013;33(2):222-32.

43) Talmant JC, Talmant JC, Lumineau JP. Traitement primaire des fentes labio-palatines. Ses grands principes [Primary treatment of cleft lip and palate. Its fundamental principles]. Ann Chir Plast Esthet. 2016;61(5):348-59. French.

44) Johnston MC, Hassell JR, Brown KS. The embryology of cleft lip and cleft palate. Clin Plast Surg. 1975;2(2):195-203.

45) Burston WR, Orth D. The development of cleft lip and palate. Ann R Coll Surg Engl. 1959;25(3):225-33.

46) Tse RW, Ettinger RE, Sitzman TJ, Mercan E. Revisiting the unrepaired unilateral cleft lip and nasal deformity using 3D surface image analysis: A data-driven model and its implications. J Plast Reconstr Aesthet Surg. 2021;74(10):2694-704.

47) Choi J, Park HS. The clinical anatomy of the maxillary artery in the pterygopalatine fossa. J Oral Maxillofac Surg. 2003;61(1):72-8.

48) von Arx T, Tamura K, Yukiya O, Lozanoff S. The face – A vascular perspective. A literature review. Swiss Dent J. 2018;128(5):382-92.

49) Moore KL, Persaud TVN, Viebahn C. Embryologie: Entwicklungsstadien – Frühentwicklung – Organogenese – Klinik. 5th ed. München: Urban & Fischer Verlag, Elsevier; 2007.

50) Hinrichsen KV, Beier HM, Breucker H, Christ B, Duncker HR, Dvorak M, von Gaudecker B, Hahn von Dorsche H, Holstein AF, Jacob HJ, Jacob M, Jorch G, Kaufmann P, Kostovic I, Prindull G, Seidl W, Steding G, Tesarik J, Wartenberg H. Humanembryologie: Lehrbuch und Atlas der vorgeburtlichen Entwicklung des Menschen. Berlin: Springer; 2014.

51) Loukas M, Hullett J, Louis RG Jr, Kapos T, Knight J, Nagy R, Marycz D. A detailed observation of variations of the facial artery, with emphasis on the superior labial artery. Surg Radiol Anat. 2006;28(3):316-24.

52) Niemann K, Lazarus L, Rennie C. An anatomical study of the facial artery. Int J Morphol. 2019;37(4):1310-15.

53) Lee KL, Lee HJ, Youn KH, Kim HJ. Positional relationship of superior and inferior labial artery by ultrasonography image analysis for safe lip augmentation procedures. Clin Anat. 2020;33(2):158-64.

54) Pinar YA, Bilge O, Govsa F. Anatomic study of the blood supply of perioral region. Clin Anat. 2005;18(5):330-9.

55) Lee SH, Gil YC, Choi YJ, Tansatit T, Kim HJ, Hu KS. Topographic anatomy of the superior labial artery for dermal filler injection. Plast Reconstr Surg. 2015;135(2):445-50.

56) Garcia de Mitchell CA, Pessa JE, Schaverien MV, Rohrich RJ. The philtrum: anatomical observations from a new perspective. Plast Reconstr Surg. 2008;122(6):1756-60.

57) Crouzet C, Fournier H, Papon X, Hentati N, Cronier P, Mercier P. Anatomy of the arterial vascularization of the lips. Surg Radiol Anat. 1998;20(4):273-8.

58) Gschwindt S, Mueller AA, Benitez BK, Baksa G, Kisnisci RS, Chong DK, Shahbazi A. Musculovascular pattern in the myrtiform area: implications for cleft lip reconstruction. Int J Oral Maxillofac Surg. 2026 Mar 25:S0901-5027(26)00092-5.

59) Jiang L, Yin N, Wang Y, Song T, Wu D, Li H. Three-dimensional visualization of blood supply of the upper lip using micro-CT and implications for plastic surgery. Clin Anat. 2021;34(2):191-8.

60) Gray H, Lewis WH. Anatomy of the Human Body. 20th ed. Philadelphia and New York: Lea & Febiger; 1918. p. 1110-2.

61) von Lanz T, Wachsmuth W. Praktische Anatomie. Vol. 1. Berlin: Springer; 1985. p. 186-8.

62) Sieglbauer F. Lehrbuch der normalen Anatomie des Menschen. 9th ed. Wien: Urban & Schwarzenberg; 1963.

63) Li KK, Meara JG, Alexander A Jr. Location of the descending palatine artery in relation to the Le Fort I osteotomy. J Oral Maxillofac Surg. 1996;54(7):822-5.

64) Kim DW, Tempski J, Surma J, Ratusznik J, Raputa W, Świerczek I, Pękala JR, Tomaszewska IM. Anatomy of the greater palatine foramen and canal and their clinical significance in relation to the greater palatine artery: a systematic review and meta-analysis. Surg Radiol Anat. 2023;45(2):101-19.

65) Choi J, Park HS. The clinical anatomy of the maxillary artery in the pterygopalatine fossa. J Oral Maxillofac Surg. 2003;61(1):72-8.

66) Benninger B, Andrews K, Carter W. Clinical measurements of hard palate and implications for subepithelial connective tissue grafts with suggestions for palatal nomenclature. J Oral Maxillofac Surg. 2012;70(1):149-53.

67) Klosek SK, Rungruang T. Anatomical study of the greater palatine artery and related structures of the palatal vault: considerations for palate as the subepithelial connective tissue graft donor site. Surg Radiol Anat. 2009;31(4):245-50.

68) Yu SK, Lee MH, Park BS, Jeon YH, Chung YY, Kim HJ. Topographical relationship of the greater palatine artery and the palatine spine: significance for periodontal surgery. J Clin Periodontol. 2014;41(9):908-13.

69) Blakeway H. Investigations in the anatomy of the palate. J Anat Physiol. 1914;48(4):409-16.

70) Shahbazi A, Grimm A, Feigl G, Gerber G, Székely AD, Molnár B, Windisch P. Analysis of blood supply in the hard palate and maxillary tuberosity–clinical implications for flap design and soft tissue graft harvesting (a human cadaver study). Clin Oral Investig. 2019;23(3):1153-60.

71) Reiser GM, Bruno JF, Mahan PE, Larkin LH. The subepithelial connective tissue graft palatal donor site: anatomic considerations for surgeons. Int J Periodontics Restorative Dent. 1996;16(2):130-7.

72) Kim DH, Won SY, Bae JH, Jung UW, Park DS, Kim HJ, Hu KS. Topography of the greater palatine artery and the palatal vault for various types of periodontal plastic surgery. Clin Anat. 2014;27(4):578-84.

73) Rossell-Perry P. Flap necrosis after palatoplasty in patients with cleft palate. Biomed Res Int. 2015;2015:516375.

74) Shahbazi A, Sculean A, Baksa G, Gschwindt S, Molnár B, Vág J, Bogdán S. Intraosseous arterial alteration of maxilla influencing implant-related surgeries. Clin Oral Investig. 2023;27(9):5217-21.

75) Iwanaga J, Takeshita Y, Anbalagan M, Zou B, Toriumi T, Kunisada Y, Ibaragi S, Tubbs RS. The greater palatine nerve and artery both supply the maxillary teeth: an anatomic and radiologic study. J Am Dent Assoc. 2025;156(2):151-159.e1.

76) Maher WP. Artery distribution in the prenatal human maxilla. Cleft Palate J. 1981;18(1):51-8.

77) Huang MHS, Lee ST, Rajendran K. Clinical implications of the velopharyngeal blood supply: a fresh cadaveric study. Plast Reconstr Surg. 1998;102(3):655-67.

78) Duisit J, Maistriaux L, Gerdom A, Vergauwen M, Gianello P, Behets C, Lengelé B. Nose and lip graft variants: a subunit anatomical study. Plast Reconstr Surg. 2018;141(3):751-61.

79) Hoke JA, Burkes EJ, White JT, Duffy MB, Klitzman B. Blood-flow mapping of oral tissues by laser Doppler flowmetry. Int J Oral Maxillofac Surg. 1994;23(5):312-5.

80) Mörmann W, Ciancio SG. Blood supply of human gingiva following periodontal surgery. A fluorescein angiographic study. J Periodontol. 1977;48(11):681-92.

81) Molnár E, Molnár B, Lohinai Z, Tóth Z, Benyó Z, Hricisák L, Windisch P, Vág J. Evaluation of laser speckle contrast imaging for the assessment of oral mucosal blood flow following periodontal plastic surgery: an exploratory study. Biomed Res Int. 2017;2017:4042902.

82) Yamamoto M, Chen HK, Hidetomo H, Watanabe A, Sakiyama K, Kim HJ, Murakami G, Rodríguez-Vázquez JF, Abe S. Superior labial artery and vein anastomosis configuration to be considered in lip augmentation. Ann Anat. 2022;239:151808.

83) Veau V. Division palatine. Anatomie, chirurgie, phonétique. Paris: Masson et Cie; 1931.

84) Tompsett DH. Anatomical techniques. 2nd ed. Edinburgh: E. & S. Livingstone; 1970.

85) Ottone NE. Brief review of the origins of anatomical techniques. In: Ottone NE, editor. Advances in plastination techniques. Cham: Springer International Publishing; 2023. p. 1-17.

86) Bedino JH. Embalming chemistry: glutaraldehyde versus formaldehyde. Champion Expanding Encyclopedia of Mortuary Practices. 2003;649:2614-32.

87) Dempster WT. Rates of penetration of fixing fluids. Am J Anat. 1960;107:59-72.

88) Chesnick IE, Mason JT, O'Leary TJ, Fowler CB. Elevated pressure improves the rate of formalin penetration while preserving tissue morphology. J Cancer. 2010;1:178-83.

89) Fox CH, Johnson FB, Whiting J, Roller PP. Formaldehyde fixation. J Histochem Cytochem. 1985;33(8):845-53.

90) Grönroos H. Zusammenstellung der üblichen Konservierungsmethoden für Präpariersaalzwecke. Anat Anz. 1898;15:61-84.

91) Suruda A. Morticians. In: Greenberg MI, Hamilton RJ, Phillips SD, McCluskey GJ, editors. Occupational, industrial, and environmental toxicology. 2nd ed. Philadelphia: Mosby Inc.; 2003. p. 274-83.

92) National Toxicology Program. Final report on carcinogens background document for formaldehyde. Rep Carcinog Backgr Doc. 2010;(10-5981):i-512.

93) Nielsen GD, Wolkoff P. Cancer effects of formaldehyde: a proposal for an indoor air guideline value. Arch Toxicol. 2010;84(6):423-46.

94) IARC Working Group on the Evaluation of Carcinogenic Risks to Humans. Formaldehyde, 2-butoxyethanol and 1-tert-butoxypropanol-2-ol. IARC Monogr Eval Carcinog Risks Hum. 2006;88:39-325.

95) Ochs M, Grotz O, Factorine LS, Rodrigues MR, Pereira Netto AD. Occupational exposure to formaldehyde in an institute of morphology in Brazil: a comparison of area and personal sampling. Environ Sci Pollut Res Int. 2011;19(7):2813-9.

96) Njoya HK, Ofusori DA, Nwangwu SC, Amegor OF, Akinyeye AJ, Abayomi TA. Histopathological effect of exposure of formaldehyde vapour on the trachea and lung of adult wistar rats. Int J Integr Biol. 2009;7(3):160-5.

97) Kiernan JA. Formaldehyde, formalin, paraformaldehyde and glutaraldehyde: what they are and what they do. Microsc Today. 2000;8(1):8-12.

98) Laskowski S. L'embaumement, la conservation des sujets et les préparations anatomiques. Genève-Bâle-Lyon: H. Georg; 1886.

99) Campbell JW, Margrave JL. Embalming composition and method. Houston: EFH Inc.; 1995.

100) Peters E. Eine verbilligte, farberhaltende Konservierungsmethode für Präparationsmaterial zu Lehr- und Übungszwecken. Anat Anz. 1956;103:89-91.

101) Pretorius W. Formula for embalming of cadavers for student dissection and the modification thereof for plastination. J Int Soc Plastination. 1996;10:35-6.

102) Richins CA, Roberts EC, Zeilmann JA. Improved fluids for anatomical embalming and storage. Anat Rec. 1963;146:241-3.

103) Thiel W. Die Konservierung ganzer Leichen in natürlichen Farben [The preservation of the whole corpse with natural color]. Ann Anat. 1992;174(3):185-95. German.

104) Kennel L, Martin DMA, Shaw H, Wilkinson T. Learning anatomy through Thiel- vs. formalin-embalmed cadavers: student perceptions of embalming methods and effect on functional anatomy knowledge. Anat Sci Educ. 2018;11(2):166-74.

105) Thiel W. Ergänzung für die Konservierung ganzer Leichen nach W. Thiel [Supplement to the conservation of an entire cadaver according to W. Thiel]. Ann Anat. 2002;184(3):267-9. German.

106) Ottone NE, Vargas CA, Fuentes R, Del Sol M. Walter Thiel's embalming method. Review of solutions and applications in different fields of biomedical research. Int J Morphol. 2016;34(4):1442-54.

107) Bertone VH, Blasi E, Ottone NE, Dominguez ML. Método de Walther Thiel para la preservación de cadáveres con mantenimiento de las principales propiedades físicas del vivo [Walther Thiel method for the preservation of corpses with maintenance of the main physical properties of vivo]. Rev Argent Anat Online. 2011;2(3):89-92. Spanish.

108) Ottone NE. Cadaveric fixation and conservation techniques prior to plastination. In: Ottone NE, editor. Advances in plastination techniques. Cham: Springer International Publishing; 2023. p. 63-83.

109) Durongphan A, Suksantilap S, Panrong N, Aungsusiripong A, Wiriya A, Pisittrakoonporn S, Pichaisak W, Pamornpol B. Latex-injected, non-decapitated,

saturated salt method-embalmed cadaver technique development and application as a head and neck surgery training model. PLoS One. 2022;17(1):e0262415.

110) Shahbazi A, Pilsl U, Molnár B, Feigl G. Detection of vascular pathways of oral mucosa influencing soft- and hard-tissue surgeries by latex milk injection. J Vis Exp. 2020;159:e60877.

111) Rueda Esteban RJ, López McCormick JS, Martínez Prieto DR, Hernández Restrepo JD. Corrosion casting, a known technique for the study and teaching of vascular and duct structure in anatomy. Int J Morphol. 2017;35(3):1147-53.

112) Verli FD, Rossi-Schneider TR, Schneider FL, Yurgel LS, de Souza MAL. Vascular corrosion casting technique steps. Scanning. 2007;29(3):128-32.

113) Lametschwandtner A, Lametschwandtner U, Weiger T. Scanning electron microscopy of vascular corrosion casts-technique and applications: updated review. Scanning Microsc. 1990;4:889-940.

114) Kishi Y, Takahashi K, Trowbridge H. Vascular network in papillae of dog oral mucosa using corrosive resin casts with scanning electron microscopy. Anat Rec. 1990;226(4):447-59.

115) Selliseth NJ, Selvig KA. Revascularization of an excisional wound in gingiva and oral mucosa. A scanning electron microscopic study using corrosion casts in rats. Scanning Microsc. 1995;9(2):455-67.

116) Hodde KC, Steeber DA, Albrecht RM. Advances in corrosion casting methods. Scanning Microsc. 1990;4(3):693-704.

117) Sims PA, Albrecht RM. Improved tissue corrosion of vascular casts: a quantitative filtration method used to compare tissue corrosion in various concentrations of sodium and potassium hydroxide. Scanning Microsc. 1993;7(2):637-42.

118) Kovacević P, Ugrenović S, Kovacević T. Vascularisation of pectoralis major myocutaneous flap: anatomical study in human fetuses and cadavers. Bosn J Basic Med Sci. 2008;8(2):183-7.

119) Wong KC, Wu LT. History of Chinese medicine. Shanghai: Mercury Press; 1936.

120) Dorrance GM. The operative story of cleft palate. Philadelphia and London: W.B. Saunders; 1933.

121) Franco P. Petit traité, contenant une des parties principales de chirurgie, laquelle les chirurgiens hernieres exercent, ainsi qu'il montre en la page suivante. 1st ed. Lyon: Antoine Vincent; 1556.

122) Dieffenbach JF. Quoted by Battersley in: The age most suitable for the operation of harelip. Lancet. 1846;2:159-160.

123) Mirault G. Deux lettres sur l'opération du bec-de-lièvre. J Chir. 1844;2:257.

124) Tennison CW. The repair of unilateral cleft lip by the stencil method. Plast Reconstr Surg. 1952;9(2):115-20.

125) Randall P. A triangular flap operation for the primary repair of unilateralclefts of the lip. Plast Reconstr Surg Transplant Bull. 1959;23(4):331-47.

126) Iliopoulos C, Mitsimponas K, Lazaridou D, Neukam FW, Stelzle F. A retrospective evaluation of the aesthetics of the nasolabial complex after unilateral cleft lip repair using the Tennison–Randall technique: a study of 44 cases treated in a single cleft center. J Craniomaxillofac Surg. 2014;42(8):1679-83.

127) Heycock MH. A field guide to cleft-lip repair. Br J Surg. 1971;58(8):567-70.

128) Meyer E, Seyfer A. Cleft lip repair: technical refinements for the wide cleft. Craniomaxillofac Trauma Reconstr. 2010;3(2):81-6.

129) Millard DR. Extensions of the rotation-advancement principle for wide unilateral cleft lips. Plast Reconstr Surg. 1968;42(6):535-44.

130) Manlove AE, Linnebur AM. Primary unilateral cleft lip repair using the modified Millard technique. Atlas Oral Maxillofac Surg Clin North Am. 2022;30(1):13-17.

131) Becker M, Svensson H, McWilliam J, Sarnäs KV, Jacobsson S. Millard repair of unilateral isolated cleft lip: a 25-year follow-up. Scand J Plast Reconstr Surg Hand Surg. 1998;32(4):387-94.

132) Saunders DE, Malek A, Karandy E. Growth of the cleft lip following a triangular flap repair. Plast Reconstr Surg. 1986;77(2):227-38.

133) Lee TJ. Upper lip measurements at the time of surgery and follow-up after modified rotation-advancement flap repair in unilateral cleft lip patients. Plast Reconstr Surg. 1999;104(4):911-5.

134) Mulliken JB, Martínez-Pérez D. The principle of rotation advancement for repair of unilateral complete cleft lip and nasal deformity: technical variations and analysis of results. Plast Reconstr Surg. 1999;104(5):1247-60.

135) Lewis MB. Unilateral cleft lip repair: Z-plasty. Clin Plast Surg. 1993;20(4):647-57.

136) Veau V, Récamier J. Bec-de-lièvre. Paris: Masson et Cie; 1938.

137) Limberg AA. Planning of local plastic operations on the body surface: theory and practice. Leningrad: Medgiz; 1963.

138) Kilner TP. Cleft lip and palate repair technique. St Thomas Hosp Rep. 1937;2:127.

139) Lemesurier AB. The operative repair of cleft palate. Can Med Assoc J. 1935;33(2):150-7.

140) Schilli W. Elektromyographische Untersuchungen bei Lippen-Kiefer-Gaumen-Spalten. Fortschr Kieferorthop. 1963;24:417-9.

141) Fára M. Pathological anatomy of the muscles in cleft lip and palate: anatomical and surgical considerations. In: Marchac D, editor. Transactions of the Sixth International Congress of Plastic and Reconstructive Surgery. Paris: Masson; 1976. p. 205-7.

142) Gundlach KK, Pfeifer G. The arrangement of muscle fibres in cleft lips. J Maxillofac Surg. 1979;7(2):109-16.

143) Kernahan DA, Dado DV, Bauer BS. The anatomy of the orbicularis oris muscle in unilateral cleft lip based on a three-dimensional histological reconstruction. Plast Reconstr Surg. 1984;73(6):875-81.

144) Delaire J, Fève JR, Chateau JP, Courtay D, Tulasne JF. Anatomie et physiologie des muscles et du frein médian de la lèvre supérieure. Premiers résultats de l'électromyographie sélective [Anatomy and physiology of the muscles and median frenum of the upper lip. Initial results of selective electromyography]. Rev Stomatol Chir Maxillofac. 1977;78(2):93-103. French.

145) Delaire J. La chéilo-rhinoplastie primaire pour fente labio-maxillaire congénitale unilatérale. Essai de schématisation d'une technique [Primary cheilorhinoplasty for congenital unilateral labiomaxillary fissure. Trial schematization of a technic]. Rev Stomatol Chir Maxillofac. 1975;76(3):193-215. French.

146) Joos U, Friedburg H. Darstellung des Verlaufs der mimischen Muskulatur in der Kernspintomographie. Fortschr Kiefer Gesichtschir. 1987;32:125-7.

147) Joos U. Skeletal growth after muscular reconstruction for cleft lip, alveolus and palate. Br J Oral Maxillofac Surg. 1995;33(3):139-44.

148) Precious DS. Unilateral cleft lip and palate. Oral Maxillofac Surg Clin North Am. 2000;12(3):399-420.

149) Letourneau A, Daniel RK. The superficial musculoaponeurotic system of the nose. Plast Reconstr Surg. 1988;82(1):48-57.

150) Figallo EE, Acosta JA. Nose muscular dynamics: the tip trigonum. Plast Reconstr Surg. 2001;108(5):1118-26.

151) Hur MS, Hu KS, Park JT, Youn KH, Kim HJ. New anatomical insight of the levator labii superioris alaeque nasi and the transverse part of the nasalis. Surg Radiol Anat. 2010;32(8):753-6.

152) Markus AF, Delaire J, Smith WP. Facial balance in cleft lip and palate. I. Normal development and cleft palate. Br J Oral Maxillofac Surg. 1992;30(5):287-95.

153) Rossell-Perry P. Atlas of operative techniques in primary cleft lip and palate repair. 1st ed. Cham: Springer; 2020.

154) Denadai R, Lo LJ. Current concept in cleft surgery: moving toward excellence of outcome and reducing the burden of care. Singapore: Springer Nature; 2022.

155) Tse RW, Fisher DM. State of the art: the unilateral cleft lip and nose deformity and anatomic subunit approximation. Plast Surg (Oakv). 2024;32(1):138-47.

156) Talmant JC. Evolution of the functional repair concept for cleft lip and palate patients. Indian J Plast Surg. 2006;39(2):196-209.

157) Talmant JC. Nasal malformations associated with unilateral cleft lip. Accurate diagnosis and management. Scand J Plast Reconstr Surg Hand Surg. 1993;27(3):183-91.

158) Joos U. Muscle reconstruction in primary cleft lip surgery. J Craniomaxillofac Surg. 1989;17 Suppl 1:8-10.

159) Pfeifer G, Pirsig W, Wulff J, Wulff H. Lippen-Kiefer-Gaumenspalten: chirurgische, otologische und sprachliche Behandlung. München: Ernst Reinhardt Verlag; 1981.

160) Pritchard JJ, Scott JH, Girgis FG. The structure and development of cranial and facial sutures. J Anat. 1956;90(1):73-86.

161) Knese KH, Geidel H. Form, Oberfläche und Volumen der Zellkerne des Periostes. Z Mikr Anat Forsch. 1972;85:223-44.

162) Ricbourg B. Vascularisation des lèvres [Blood supply of the lips]. Ann Chir Plast Esthet. 2002;47(5):346-56. French.

163) Salmon M. Artères des muscles de la tête et du cou. Paris: Masson; 1936. p. 9-75.

164) Mitz V, Ricbourg B, Lassau JP. Les branches faciales de l'artère faciale chez l'adulte. Typologie, variations et territoires cutanés respectifs [Facial branches of the facial artery in adults. Typology, variations and respective cutaneous areas]. Ann Chir Plast. 1973;18(4):339-50. French.

165) Rossell-Perry P. Atlas of non-desirable outcomes in cleft lip and palate surgery: A case-based guide to preventing and managing complications. 1st ed. Cham: Springer; 2022.

166) Shahbazi A, Mueller AA, Mezey S, Gschwindt S, Kiss T, Baksa G, Kisnisci RS. Is the collateral circulation pattern in the hard palate affected by cleft deformity? Clin Oral Investig. 2024;28(5):277.

167) Maher WP. Distribution of palatal and other arteries in cleft and non-cleft human palates. Cleft Palate J. 1977;14(1):1-12.

168) Wilhelm R. Die chirurgische Anatomie der Gefäss- und Nervenversorgung des harten und weichen Gaumens bei Neugeborenen unter der Berücksichtigung operativer Eingriffe. Wissenschaftliche Zeitschrift der Friedrich-Schiller-Universität Jena/Thüringen. 1969;815-18.

169) Gauthier A, Lézy JP, Vacher C. Vascularization of the palate in maxillary osteotomies: anatomical study. Surg Radiol Anat. 2002;24(1):13-7.

170) Teemul TA, Perfettini J, Morris DO, Russell JL. Post-operative avascular necrosis of the maxilla: a rare complication following orthognathic surgery. J Surg Case Rep. 2017;2017(1):rjw240.

171) Heggie A, Robertson K, Shand J. Avascular necrosis in cleft maxillary repositioning: a review of cases and introduction of the “delayed maxillary flap.” Int J Oral Maxillofac Surg. 2021;50(2):185-90.

172) Ogata H, Sakamoto Y, Kishi K. Cleft palate repair without lateral relaxing incision. Plast Reconstr Surg Glob Open. 2017;5(3):e1256.

173) Bosma JF. Anatomy of the infant head. Baltimore: Johns Hopkins University Press; 1986.

174) Von Langenbeck B. Operation der angeborenen totalen Spaltung des harten Gaumens nach einer neuen Methode. Dtsch Klin. 1861;13:231; also Plast Reconstr Surg. 1972;49:323-4.

175) Delaire J, Mercier J, Gordeeff A, Bedhet N. Les trois fibro-muqueuses palatines. Leur rôle dans la croissance du maxillaire. Déductions thérapeutiques dans la chirurgie des divisions palatines [The 3 palatine fibromucous membranes. Their role in maxillary growth. Therapeutic role in surgery of the palatine shelves]. Rev Stomatol Chir Maxillofac. 1989;90(6):379-90. French.

176) Murison MS, Pigott RW. Medial Langenbeck: experience of a modified Von Langenbeck repair of the cleft palate. A preliminary report. Br J Plast Surg. 1992;45(6):454-9.

177) Markus AF, Smith WP, Delaire J. Primary closure of cleft palate: a functional approach. Br J Oral Maxillofac Surg. 1993;31(2):71-7.

178) Wardill WEM. The technique of operation for cleft palate. Br J Surg. 1937;25(97):117-30.

179) Cuthbert J. Transposed flaps in cleft palate repair. Br J Plast Surg. 1951;4(3):185-7.

180) Perko MA. Primary closure of the cleft palate using a palatal mucosal flap: an attempt to prevent growth impairment. J Maxillofac Surg. 1974;2(1):40-3.

181) Bardach J. Two-flap palatoplasty: Bardach's technique. Operat Tech Plast Reconstr Surg. 1995;2(4):211-14.

182) Dieffenbach FJ. Beiträge zur Gaumennath. Litt Ann Heilk. 1826;6:305.

183) Shetty V, Sreekumar C, Patteta NK, Bahl D, Sailer HF. Correlation between surgical protocols for palatoplasty and midfacial growth in cleft lip and palate patients: a long-term, single-centre study. J Craniomaxillofac Surg. 2021;49(11):1010-19.

9. Bibliography of the candidate's publications

1) Shahbazi A, Sculean A, Baksa G, **Gschwindt S**, Molnár B, Vág J, Bogdán S. Intraosseous arterial alteration of maxilla influencing implant-related surgeries. Clin Oral Investig. 2023;27(9):5217-5221.
(Journal: Clinical Oral Investigations; Rank: D1; Impact factor: 3,1)

2) Shahbazi A, Mueller AA, Mezey S, **Gschwindt S**, Kiss T, Baksa G, Kisnisci RS. Is the collateral circulation pattern in the hard palate affected by cleft deformity? Clin Oral Investig. 2024;28(5):277.
(Journal: Clinical Oral Investigations; Rank: D1; Impact factor: 3,1)

3) **Gschwindt S**, Mueller AA, Benitez BK, Baksa G, Kisnisci RS, Chong DK, Shahbazi A. Musculovascular pattern in the myrtiform area: implications for cleft lip reconstruction. Int J Oral Maxillofac Surg. 2026 Mar 25:S0901-5027(26)00092-5.
(Journal: International Journal of Oral and Maxillofacial Surgery; Rank: Q1; Impact factor: 2,7)

10. Acknowledgements

I want to express my deepest gratitude to Dr. Arvin Shahbazi for his guidance and mentorship throughout my PhD journey. His support extended far beyond what is expected of a supervisor, a commitment I had already experienced during my medical studies. He consistently provided clear feedback, constructive criticism and fostered an encouraging environment that not only strengthened the quality of our collaborative work but also helped me grow as a researcher. His generosity with his time, his patience in addressing challenges, and his ability to create an atmosphere in which ideas could develop and improve. I am profoundly grateful for his dedication, which has shaped both the outcome of this thesis and my academic path.

I would like to extend a very special thank you to Dr. Tamás Ruttkay and Dr. Gábor Baksa for their organization and continuous support. My sincere thanks also go to the Department of Anatomy, Histology and Embryology, and most importantly, to all the individuals who generously donated their bodies to medical education and research.
The quality of our research would not have been possible without the valuable contributions of our research collaborators. Their expertise, dedication, and willingness to share ideas enriched our projects in numerous ways.

Finally, I would like to thank my parents for their unwavering love, encouragement, and support. Their belief in me has been a constant source of strength and motivation throughout my dental, medical and PhD studies.